

AD-A128 483

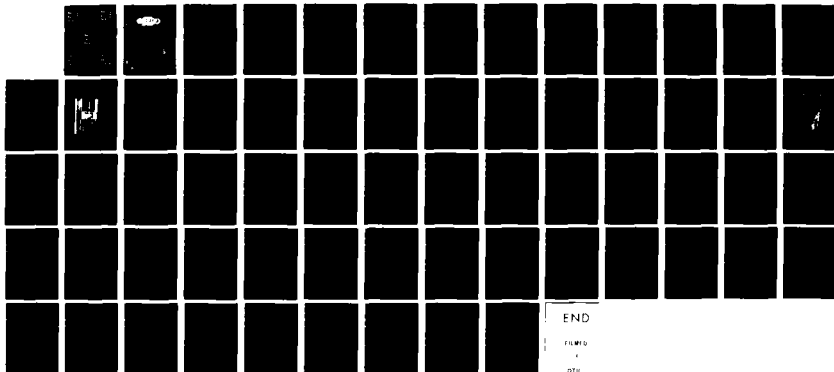
A STUDY OF COLORS IN LUTETIUM DIPTHALOCYANINE  
ELECTROCHROMIC DISPLAYS(U) ROCKWELL INTERNATIONAL  
ANAHEIM CA AUTONETICS STRATEGIC SYSTEM.  
M M NICHOLSON ET AL. OCT 82 C82-268/201

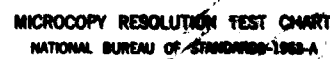
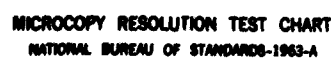
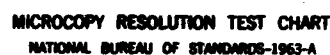
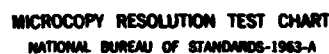
1/1

UNCLASSIFIED

F/G 7/4

NL





AD A120483

C82-268/201

12



## A STUDY OF COLORS IN LUTETIUM DIPHETHALOCYANINE ELECTROCHROMIC DISPLAYS

Colors of lutetium diphthalocyanine  
electrochromic films were fundamentally correlated with  
applied voltage and electrolyte acidity.

**M. M. NICHOLSON  
T. P. WEISMULLER**

**ROCKWELL INTERNATIONAL CORPORATION  
ANAHEIM  
CALIFORNIA  
92803**

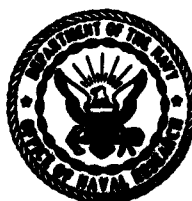
**CONTRACT N00014-81-C-0284**

**OCTOBER 1982**

**DTIC  
ELECTE  
S OCT 19 1982 D  
F**

**FINAL REPORT FOR PERIOD 15 FEBRUARY 1981 TO 14 FEBRUARY 1982**

**Approved for public release, distribution unlimited.**



**PREPARED FOR THE  
OFFICE OF NAVAL RESEARCH • 800 N. QUINCY ST. • ARLINGTON, VA. 22217**

**82 10 19 009**

DTIC FILE COPY

Unclassified

SECURITY CLASSIFICATION OF THIS PAGE (When Data Entered)

REPORT DOCUMENTATION PAGE		READ INSTRUCTIONS BEFORE COMPLETING FORM
1. REPORT NUMBER	2. GOVT ACCESSION NO. <b>AD-A120483</b>	3. RECIPIENT'S CATALOG NUMBER
4. TITLE (and Subtitle) <b>A Study of Colors in Lutetium Diphthalocyanine Electrochromic Displays</b>		5. TYPE OF REPORT & PERIOD COVERED <b>Final, 15 February 1981 to 14 February 1982</b>
7. AUTHOR(s) <b>M. M. Nicholson T. P. Weismuller</b>		6. PERFORMING ORG. REPORT NUMBER <b>C82-268/201</b>
9. PERFORMING ORGANIZATION NAME AND ADDRESS <b>Autonetics Strategic Systems Division Rockwell International Anaheim, California 92803</b>		8. CONTRACT OR GRANT NUMBER(s) <b>N00014-81-C-0264</b>
11. CONTROLLING OFFICE NAME AND ADDRESS <b>Office of Naval Research Arlington, Virginia 22217</b>		10. PROGRAM ELEMENT, PROJECT, TASK AREA & WORK UNIT NUMBERS
14. MONITORING AGENCY NAME & ADDRESS (if different from Controlling Office)		12. REPORT DATE <b>October 1982</b>
		13. NUMBER OF PAGES <b>60</b>
		15. SECURITY CLASS. (of this report) <b>Unclassified</b>
		15a. DECLASSIFICATION/DOWNGRADING SCHEDULE
16. DISTRIBUTION STATEMENT (of this Report)  <b>Approved for public release; distribution unlimited.</b>		
17. DISTRIBUTION STATEMENT (of the abstract entered in Block 20, if different from Report)		
18. SUPPLEMENTARY NOTES		
19. KEY WORDS (Continue on reverse side if necessary and identify by block number) <b>Electrochromic Displays Color Phthalocyanines Rare Earths</b>		
20. ABSTRACT (Continue on reverse side if necessary and identify by block number) <b>The rare-earth diphthalocyanines have potential applications in flat-panel multicolor displays for military purposes. Lutetium diphthalocyanine electrochromic films were investigated in oxygen-free chloride solutions from pH 1 to 7 by spectroelectrochemical methods under near-equilibrium conditions. Colors are reported in CIE and Munsell notations calculated from absorption spectra. The results include a comprehensive pH-potential-color diagram and a unified scheme for the electrochemical reactions of the display material. Stability zones are defined for the principal colors</b>		

DD FORM 1 JAN 73 1473

EDITION OF 1 NOV 65 IS OBSOLETE

Unclassified  
SECURITY CLASSIFICATION OF THIS PAGE (When Data Entered)

Unclassified

SECURITY CLASSIFICATION OF THIS PAGE(When Data Entered)

orange, green, light blue (two types), dark purple-blue, and violet. Yellows, blue-greens, and additional dark blues are shown to result from blending pairs of principal colors in specified proportions. Other color modifications arising from discontinuities in the electrochromic film are treated in terms of a mathematical model. The results and methodology of this study will be useful in further work to optimize the display colors and extend the cycle life. ←

Accession For	
NTIS GRA&I	<input checked="checked" type="checkbox"/>
DTIC TAB	<input type="checkbox"/>
Unannounced	<input type="checkbox"/>
Justification	
By	
Distribution/	
Availability Codes	
Dist	Avail and/or Special
A	



Unclassified

SECURITY CLASSIFICATION OF THIS PAGE(When Data Entered)

## CONTENTS

	Page
I. INTRODUCTION . . . . .	1
II. EXPERIMENTAL PROCEDURES . . . . .	3
A. Materials . . . . .	3
B. Experimental Cells . . . . .	6
C. Measurements . . . . .	8
D. Computations . . . . .	8
III. RESULTS AND DISCUSSION . . . . .	9
A. Characterization of Colors . . . . .	9
1. Absorption Spectra . . . . .	10
2. Conversion of Spectra to Colors . . . . .	10
3. Principal Colors . . . . .	16
B. pH-Potential-Color Relationships . . . . .	18
1. Pourbaix Diagrams . . . . .	18
2. The Lutetium Diphthalocyanine Diagram . . . . .	20
3. Implications for Display Performance . . . . .	21
4. Fundamental Interpretations . . . . .	23
C. Electrochemical Reactions . . . . .	29
1. $n$ Values and Chemical Equations . . . . .	29
2. Comparisons with Previous Results . . . . .	33
D. Modified Colors . . . . .	35
1. Blended Colors . . . . .	35
2. Discontinuous Films . . . . .	41
E. Supplementary Items in Colors . . . . .	48
IV. CONCLUSIONS . . . . .	50
V. ACKNOWLEDGMENTS . . . . .	51
VI. REFERENCES . . . . .	52

## TABLES

		Page
1.	Dye Electrodes . . . . .	4
2.	Electrolytes . . . . .	5
3.	Transformation of Visible Spectrum to CIE and Munsell Color Notations . . . . .	15
4.	Principal Colors of Lutetium Diphthalocyanine Film in Oxygen- Free Electrolytes Containing Chloride Ion . . . . .	17
5.	Faradaic n Values for Electrochromic Transitions of Lutetium Diphthalocyanine . . . . .	31
6.	Transitional Colors in the Lutetium Diphthalocyanine System . . . . .	36

## FIGURES

	Page
1. Experimental Cell . . . . .	7
2. Absorption Spectra in the Orange/Green System . . . . .	11
3. Absorption Spectra in the Green/Light Blue System . . . . .	12
4. Absorption Spectra in the Light Blue/Violet System . . . . .	13
5. pH-Potential-Color Diagram . . . . .	19
6. Dependence of Orange-Film Absorption-Peak Height on pH . . .	22
7. Dependence of Cycled Green-Film Absorption-Peak Height on pH . . . . .	24
8. Spectra of Light Blue Films at Different pH Values . . . . .	25
9. Spectra Observed within Dark Purple-Blue Region of pH- Potential Diagram . . . . .	26
10. Comparison of Spectra for Violet Films at pH > 4 and pH < 4 . . . . .	28
11. Determination of Switching Charge for Green-to-Orange Transition by Incremental Voltage Steps . . . . .	30
12. Dependence of Apparent n Value on Voltage Increment for the Light Blue/Dark Purple-Blue Transition in 0.1 M HCl . . . . .	32
13. Computer Blending of Orange and Green to Grayish Yellow . . .	38
14. Computer Blending of Green and Light Blue to Blue-Green . . .	39
15. Computer Blending of Light Blue and Violet to Dark Purple-Blue . . . . .	40
16. Models for Discontinuous Films with 75 Percent Surface Coverage . . . . .	43
17. Relation of Observed Absorbance of Discontinuous Film to True Absorbance of Continuous Film . . . . .	45
18. Spectra of Initial, Cycled, and Mathematically Reconstructed Green Film . . . . .	46

## FIGURES (Continued)

	Page
19. Recorded and Reconstructed Spectra of Cycled Orange Film . . .	47
20. Observed and Mathematically Attenuated Spectra of Violet Films, Corresponding to Gray at 20 Percent Discontinuity . . .	49

## I. INTRODUCTION

Flat-panel color displays are needed for military applications ranging from hand-carried information systems to cockpit advisory and large-screen status displays. Through several years of research, spearheaded by Rockwell International, it has been shown that a multicolor electrochromic technology based on the rare-earth diphthalocyanine dyes offers exceptional promise for such applications.<sup>(1-15)</sup> A film of a single compound within this series produces several discrete, or principal colors, as well as intermediate ones, in response to variation of a low input dc voltage. Once an image is formed, it will remain, even with the display electrode on open circuit. The image is erased or modified by applying another voltage signal. The switching mechanism is similar to charging a battery, but since the electrochromic film is very thin, the energy is only a few millijoules per square centimeter. Like a battery, the display contains a liquid electrolyte and a counter electrode which carries the current through the other side of the cell. Designs of model display cells are given, for example, in Reference 9. The display may be front or back-lighted, and it may be projected on a screen. Since the display effect is based on light absorption rather than emission, the image is easily seen in bright sunlight. There is no angular viewing problem. The natural time constant of the electrochromic process is of the order of 10 ms,<sup>(9)</sup> and rapid switching persists, in a low-freezing electrolyte, at a temperature as low as -50°C.<sup>(9)</sup> A very recent paper by Bessonat *et al.* reported a life of  $2 \times 10^7$  cycles for green/red switching of lutetium diphthalocyanine and  $10^5$  cycles for green/purple, both in aqueous sulfuric acid.<sup>(14)</sup>

This exceptional combination of display characteristics makes the diphthalocyanine technology a strong potential candidate to replace CRT's in many types of information displays. However, more development work is required to optimize the performance of the electrochromic material and incorporate it in fieldable military hardware.

The present study was undertaken to characterize the lutetium diphthalocyanine colors in more detail and provide approaches for color optimization. We had observed previously that the green/red transition

depended on the electrolyte anion but apparently not on the pH,\* while processes in the green/blue-to-violet region were pH-dependent.<sup>(11)</sup> The investigation of pH effects on the electrochromic system was therefore of prime importance. A further purpose was to determine whether a yellow mode of the dye was a discrete chemical state or a mixture of chemical forms. Finally, the information on colors and their stability ranges was expected to lead toward displays of longer cycle life. All of these objectives were accomplished.

This report characterizes in detail the principal colors and various blended colors obtainable with lutetium diphthalocyanine films in deaerated chloride electrolytes at pH 1 to 7. Optical absorption spectra were recorded at small voltage intervals with the dye electrode essentially at electrochemical equilibrium. The charge uptake associated with the incremental voltage steps also could be measured.

The results include a comprehensive pH-potential-color correlation scheme which defines preferred operating conditions for the display. Effects of early-stage electrical cycling on the color quality of the films were also examined. This led to a mathematical model for discontinuous dye films that accounts for certain observed color modifications and enables the prediction of other variations not yet observed.

---

\*pH is a chemical notation for acidity on an inverse logarithmic scale. Pure water has a pH of 7, and more acidic solutions have lower pH values.

## II. EXPERIMENTAL PROCEDURES

### A. MATERIALS

Lutetium diphthalocyanine was prepared by the method of Moskalev and Kirin, as described in a previous report,<sup>(1)</sup> and thermally sublimed under vacuum to form the dye electrodes. The weight of dye per unit area was known from the optical absorbance maximum of the film near 665 nm.<sup>(1)</sup> At a maximum of 2.00, the film contained  $29.0 \mu\text{g}/\text{cm}^2$  of lutetium diphthalocyanine and was approximately 1,800 Å thick. The transparent conductive substrate in most experiments was tin oxide/glass from Corning Glass Works, prepared by a pyrolytic fog process. It had a sheet resistivity of 21-24 ohms/square. A few measurements were made with substrates of commercial sputtered tin oxide (43 ohms/square) and an experimental sputtered indium oxide (100 ohms/square). The substrate resistivities were verified by the 4-point probe method. Characteristics of the dye electrodes are listed in Table 1.

Silver-silver chloride reference and counter electrodes were prepared by anodizing silver foil in 1 M KCl.

The electrolytes, which included buffers ranging from pH 1.3 to 7.2, were water solutions of reagent grade chemicals. The electrolyte compositions and pH values determined at 25°C are given in Table 2.

TABLE 1  
DYE ELECTRODES

A. SPRAYED TIN OXIDE SUBSTRATE (21-24 OHMS/SQUARE)<sup>a</sup>

No.	$A_{\max}$ (Initial Green)	No.	$A_{\max}$ (Initial Green)	No.	$A_{\max}$ (Initial Green)
1	0.92	9	1.92	16	1.62
2	0.93	10	1.92	17	1.61
3	1.86	11	1.95	18	1.77
4	2.41	12	1.96	19	1.77
5	2.41	13	1.97	20	1.81
6	2.42	14	1.98	21	1.83
7	2.45	15	2.02		
8	2.88				

B. SPUTTERED TIN OXIDE SUBSTRATE (43 OHMS/SQUARE)

No.	$A_{\max}$ (Initial Green)
22	1.21
23	1.22

C. SPUTTERED INDIUM OXIDE SUBSTRATE (100 OHMS/SQUARE)

No.	$A_{\max}$ (Initial Green)
24	1.08
25	1.14
26	1.24
27	1.20

<sup>a</sup>Corning pyrolytic fog process

TABLE 2  
ELECTROLYTES<sup>a</sup>

pH	Components (moles/l)				
	KCl	HCl	KHC <sub>8</sub> H <sub>4</sub> O <sub>4</sub>	KH <sub>2</sub> PO <sub>4</sub>	NaOH
~1	0	0.1	0	0	0
1.3	1.0	0.097	0	0	0
1.9	1.0	0.0106	0	0	0
3.0	1.0	0.0203	0.050	0	0
4.2	1.0	0	0.050	0	0.0004
5.2	1.0	0	0.050	0	0.0239
6.1	1.0	0	0	0.050	0.0057
7.2	1.0	0	0	0.050	0.0296
~7	1.0	0	0	0	0

<sup>a</sup>Electrolytes at pH 1.3 to 7.2 were also prepared without KCl. These are designated as low-chloride or chloride-free solutions in the figures and text.

## B. EXPERIMENTAL CELLS

Figure 1 shows a photograph of an experimental cell with components and design features indicated. The housing was a Klett colorimeter cell constructed of optical glass appropriate for spectrophotometric measurements. Each cell contained a test electrode with a known area of dye film in the range of 1.4 to 2.1 cm<sup>2</sup> exposed to the solution. Electrical contact to the dye plate was made with du Pont conductive silver paste. The upper portion of the plate and its electrical contact were insulated with Apiezon W-100 wax. This wax also formed the seal to the plastic cell cover and the seals around the electrode leads. In addition to the dye electrode, the cell contained a counter electrode, which carried the same current, and a reference electrode connected in a very high-resistance potentiometric circuit. This reference served to establish the electrochemical potential of the dye electrode. All potentials are reported on the Ag/AgCl, Cl<sup>-</sup>(1 M) scale.

The electrolytes were deaerated by the passage of high-purity helium and then transferred in sealed containers to a helium-atmosphere glove box in which the oxygen level did not exceed a few parts per million. The cells were filled with the oxygen-free electrolyte and sealed inside the glove box.



Figure 1. Experimental Cell

### C. MEASUREMENTS

A sealed cell was removed from the glove box and placed in the sample beam of a Beckman Model 5230 Spectrophotometer. Small-diameter wires to the electrodes were inserted under the edges of the sample-compartment cover without causing leakage of light. A blank cell containing the electrolyte and conductive substrate without a dye deposit was placed in the reference beam.

Electrochemical measurements were made with a Princeton Applied Research Model 173 Potentiostat/Galvanostat equipped with a Model 179 Coulometer and Model 175 Universal Programmer. The principal technique consisted of in situ recording of the absorption spectrum from 350 to 800 nm while the dye electrode was held at a known potential under essentially zero current. This near-equilibrium condition was achieved by changing the voltage in small incremental steps, usually  $\leq 0.1$  V, and allowing up to several minutes for the charge to reach a constant level on the pen recorder. A close approach to zero current for the dye was confirmed by constancy of the absorption spectrum. Faradaic  $n$  values for the electrochromic transitions were evaluated by summing the incremental charges over the corresponding voltage ranges.

Voltage limits imposed by electrolysis of the solutions were determined on blank electrodes by linear potential-sweep voltammetry. The anodic and cathodic decomposition potentials were found in a conventional manner by extrapolating the steeply rising end-range currents to their intersections with the voltage axis. The voltammograms were recorded at a full-scale current sensitivity corresponding to approximately  $500 \mu\text{A}/\text{cm}^2$  on the blank electrodes.

### D. COMPUTATIONS

Spectral data were converted to CIE color notations by use of a Commodore Super PET computer. Details are given in Section III-A-2.

### III. RESULTS AND DISCUSSION

In Part A of this section, principal colors of the lutetium diphthalocyanine system are characterized by detailed analysis of spectral data. Important pH-potential-color relationships are developed in Part B, and their implications for display performance are discussed. In Part C, these relationships are further used, in conjunction with charge data, to formulate an electrochemical reaction scheme for the dye in acidic chloride electrolytes. Two types of modified colors are treated quantitatively in Part D. The first type is derived by blending the principal colors, while the second arises from discontinuities in the dye film. Finally, the availability of full-color items supplementing this report is noted in Part E.

#### A. CHARACTERIZATION OF COLORS

A vacuum-deposited film of lutetium diphthalocyanine is initially green. Near pH 7, its open-circuit potential usually is in the range of  $0.0 \pm 0.2$  V on the Ag/AgCl scale.<sup>(1)</sup> Electrochemical oxidation of the dye occurs at positive potentials, with a color change from green to orange or red. At negative potentials, reduction to light blue is first observed. As the potential is made still more negative, the color is transformed to dark blue, and finally to violet. The dye molecule loses electrons and gains a compensating number of anions when it is oxidized; it gains electrons and cations when it is reduced. Conversion to the darkest blue, or purple-blue, is promoted by acidic electrolytes.<sup>(11)</sup> Such colors, except the darkest ones, were documented previously, through visual matching with Munsell standards, in a Navy contract report.<sup>(1)</sup> The electrolyte in that case was unbuffered 0.1 M KCl, and the cell was open to the air. This investigation used other electrolytes in sealed cells. Colors are reported in the Munsell notations, but the matching was done by mathematical analysis of absorption spectra, rather than visual observation. This provided quantitative detail and allowed the color capability of the system to be more thoroughly explored.

## 1. Absorption Spectra

Recorded spectra spanning the major transition regions in air-free buffered 1 M KCl are shown in Figures 2-4. Many spectra were obtained, but only selected examples illustrating significant features are included in the report.

Isosbestic (common intersection) points are indicated for the orange/green, green/light blue, and light blue/purple blue (or violet) transitions. Such points were confirmed in related spectra (not shown) taken at 0.1-V intervals in 0.1 M HCl. The intersections in those curves were at 568 and 686 nm for orange/green, at 403, 559, and 667 nm for green/light blue, and at 385, 607, and 750 nm for light blue/purple-blue. The occurrence of isosbestic points is consistent with a clear-cut reaction stoichiometry for the transition. In this respect, the orange/green processes observed here with air absent appeared simpler than the red/green conversion reported previously for dye/tin oxide electrodes in the presence of air.<sup>(1)</sup>

Some comparison spectra were recorded for dye films deposited on  $\text{In}_2\text{O}_3$ /glass, and  $\text{SnO}_2$  sputtered on glass. These proved not to be significantly different in appearance from the spectra recorded for the Corning  $\text{SnO}_2$ /glass electrodes. However, some difficulty was encountered in fully converting the dye on  $\text{In}_2\text{O}_3$  from one color to another, possibly due to a defective deposition of the substrate.

## 2. Conversion of Spectra to Colors

Several systems for the quantitative characterization of colors have been established from the visual responses of many human observers.<sup>(16-18)</sup> The Commission Internationale de l'Eclairage (CIE) system is well adapted for the transformation of a reflectance or transmittance spectrum to a set of three color coordinates. The Munsell system uses a different color notation which is easily associated with the visual effect. It has the further advantage that standard color samples may be purchased for a wide range of Munsell colors.<sup>(19)</sup> Both the CIE and Munsell systems were used in this investigation to transform the absorption spectra to color notations and viewable colors. The procedure was as follows:

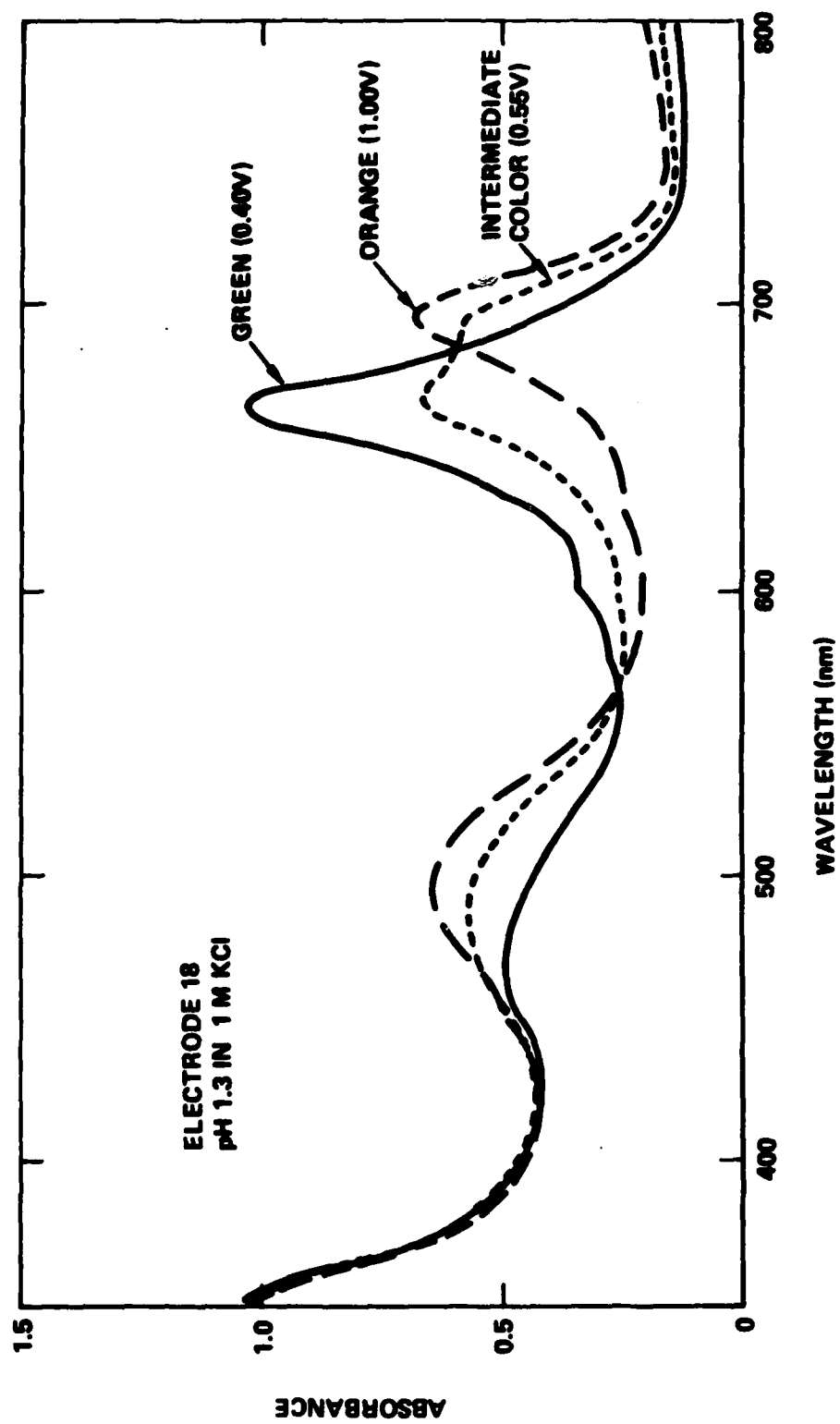


Figure 2. Absorption Spectra in the Orange/Green System

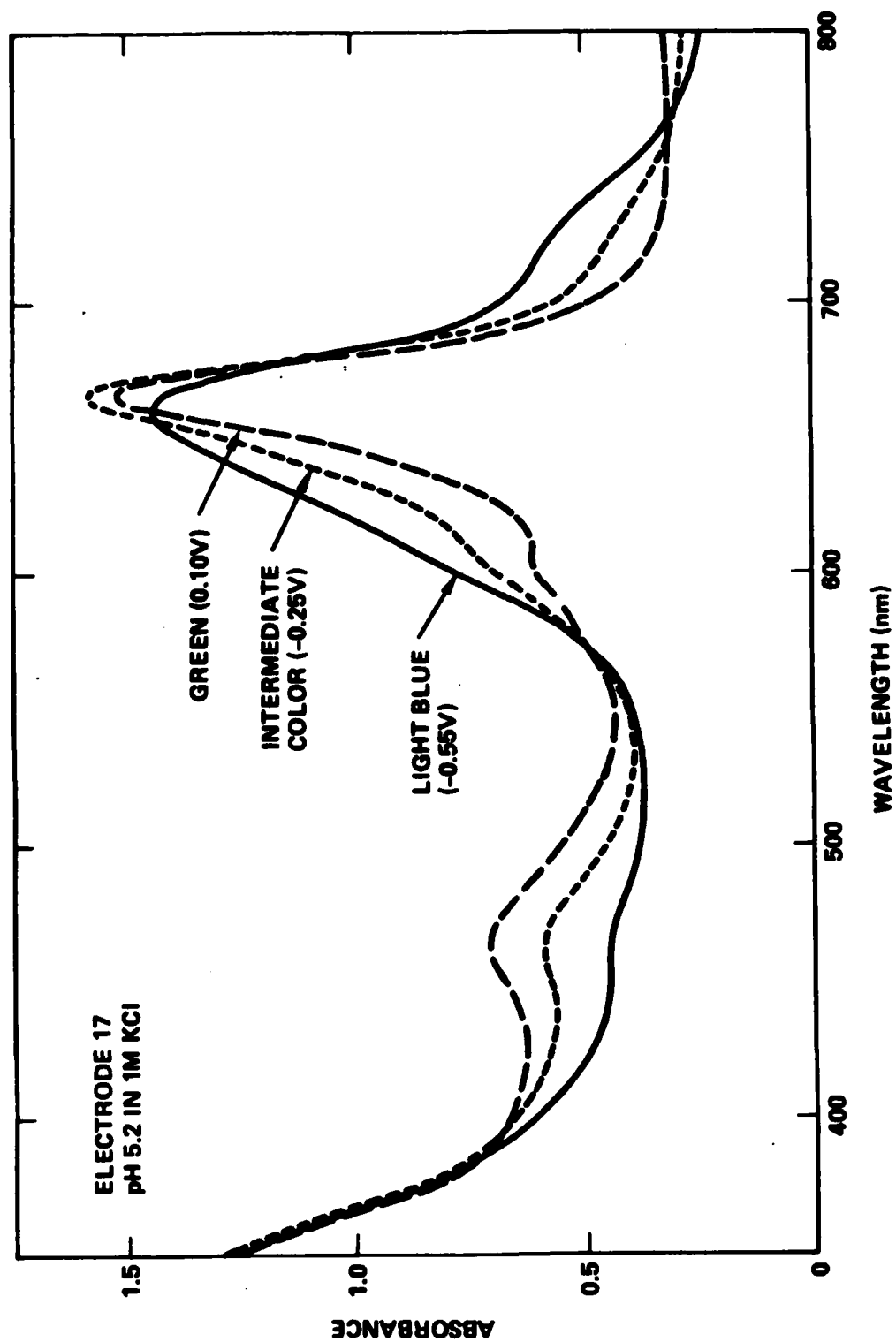


Figure 3. Absorption Spectra in the Green/Light Blue System

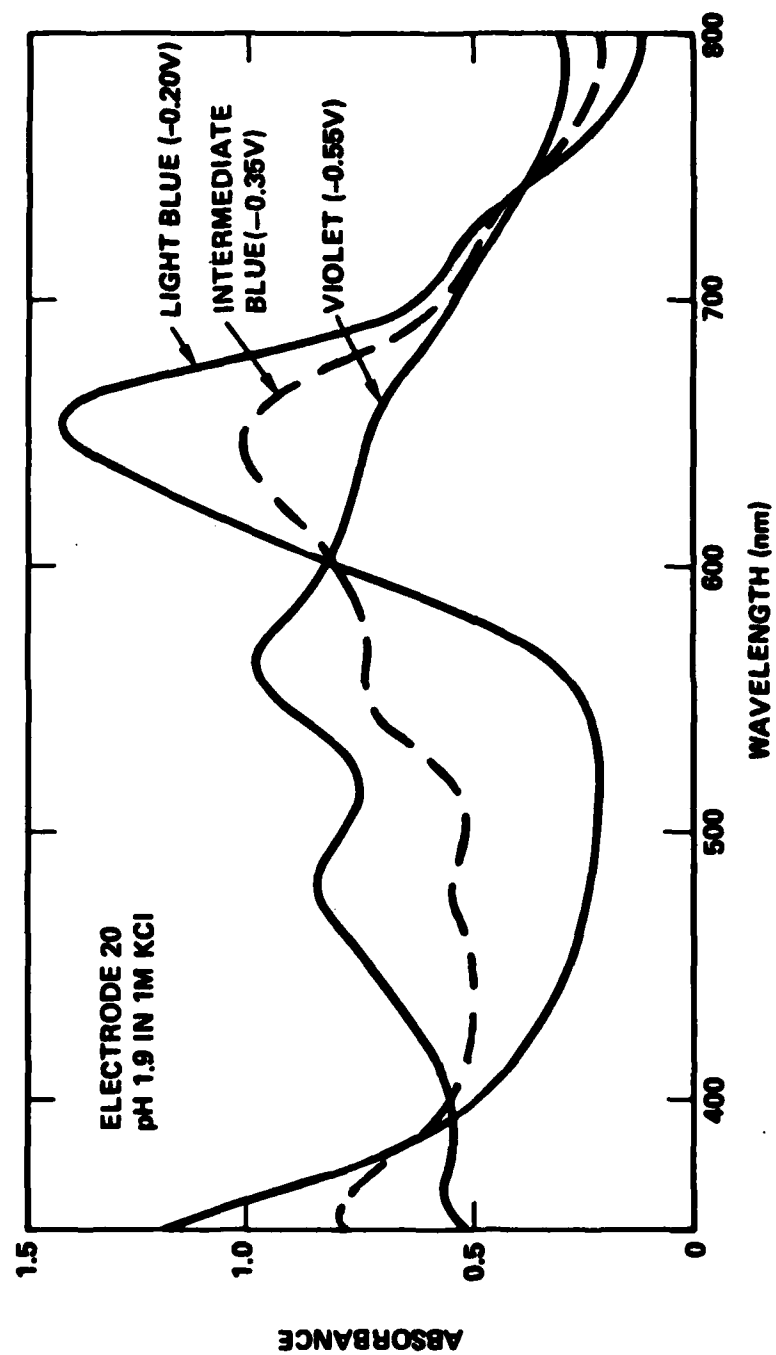


Figure 4. Absorption Spectra in the Light Blue/Violet System

CIE chromaticity coordinates  $x$ ,  $y$ , and  $z$  were obtained by analysis of the absorption spectrum with the ten-selected-ordinate method described, for example, by Trujillo.<sup>(18)</sup> Table 3 gives details of the color calculation for an uncycled vacuum-deposited "initial green" film of lutetium diphthalocyanine. The absorbance  $A$  was first read for three sets of wavelengths within the visible region. Each set contained ten wavelengths specified for the CIE system. To express the results in terms of a standard dye-film thickness, the measured absorbance  $A$  at each point was multiplied by the factor  $2.000/A_{\max}$  where  $A_{\max}$  is the observed maximum absorbance near 665 nm for the initial green film. In the example of Table 3,  $A_{\max}$  was 1.62. Thus, the adjusted absorbance  $A^*$  at any wavelength is

$$A^* = A(2.000/A_{\max}) \quad (1)$$

This standard was chosen because a lutetium diphthalocyanine film with a maximum absorbance of 2 in the initial green state produces intense colors appropriate for a back-lighted or projected display.

The adjusted absorbance was then converted to transmittance; the transmittances were summed; and the sums were multiplied by standard factors peculiar to the ten-ordinate method. This yielded the CIE tristimulus values  $X$ ,  $Y$ , and  $Z$  shown in the table. The chromaticity coordinates  $x$ ,  $y$ , and  $z$  are normalized versions of  $X$ ,  $Y$ , and  $Z$ , such that

$$x + y + z = 1 \quad (2)$$

The procedure used for converting a CIE color to the Munsell system was that given in ASTM Designation D 1535-68.<sup>(17)</sup> The  $Y$  tristimulus value was first correlated with a Munsell value  $V_y$ . Coordinates  $x$  and  $y$  were then located on the appropriate value tables of the Designation, and the corresponding Munsell color notation was found by interpolation. For the example in Table 3,  $V_y$  was 6.89, and the final Munsell notation was as follows:

	Hue	Value/Chroma
Interpolated	2.4G	6.9/8.0
Nearest Chip in Munsell Book <sup>(19)</sup>	2.5G	7/8

TABLE 3

## TRANSFORMATION OF VISIBLE SPECTRUM TO CIE AND MUNSELL COLOR NOTATIONS

Example: Dry Vacuum Deposited Initial Green Film (Electrode 16)

X Ordinates				Y Ordinates				Z Ordinates			
Wavelength (nm)	A <sub>x</sub>	A <sub>x</sub> <sup>*</sup>	T <sub>x</sub> <sup>*</sup>	Wavelength (nm)	A <sub>y</sub>	A <sub>y</sub> <sup>*</sup>	T <sub>y</sub> <sup>*</sup>	Wavelength (nm)	A <sub>z</sub>	A <sub>z</sub> <sup>*</sup>	T <sub>z</sub> <sup>*</sup>
435.5	0.488	0.602	0.250	489.4	0.368	0.454	0.352	422.2	0.492	0.607	0.247
461.2	0.548	0.677	0.210	515.1	0.230	0.284	0.520	432.0	0.489	0.604	0.249
544.3	0.202	0.249	0.574	529.8	0.202	0.249	0.564	438.6	0.490	0.605	0.248
564.1	0.281	0.347	0.450	541.4	0.202	0.249	0.564	444.4	0.498	0.615	0.243
577.3	0.326	0.402	0.396	551.8	0.217	0.268	0.540	450.1	0.515	0.636	0.231
588.7	0.419	0.517	0.304	561.9	0.259	0.320	0.479	455.9	0.542	0.669	0.214
599.6	0.493	0.609	0.246	572.5	0.332	0.410	0.389	462.0	0.548	0.677	0.210
610.9	0.497	0.614	0.243	584.8	0.392	0.484	0.328	468.7	0.530	0.654	0.222
624.2	0.570	0.704	0.198	600.8	0.496	0.612	0.244	477.7	0.460	0.568	0.270
645.9	1.050	1.296	0.051	627.3	0.614	0.758	0.175	495.2	0.329	0.406	0.393
$\Sigma T_x^* = 2.922$				$\Sigma T_y^* = 4.155$				$\Sigma T_z^* = 2.527$			

 $A_j$  = measured absorbance ( $j = x, y, \text{ or } z$ ) $A_j^*$  = absorbance adjusted to  $A_{\max} = 2.000$  for initial green $T_j^*$  = transmittance  $T_j^* = 10^{-A_j^*}$  $x = 0.09804 \Sigma T_x^* = 0.2865$  $x = X/(X + Y + Z)$  $= 0.2864$  $y = 0.1000 \Sigma T_y^* = 0.4155$  $y = Y/(X + Y + Z)$  $= 0.4153$  $z = 0.11812 \Sigma T_z^* = 0.2985$  $z = Z/(X + Y + Z)$  $= 0.2984$ 

From ASTM Designation D 1535-68, the Munsell notation corresponding to  $Y = 0.4155$ ,  $x = 0.2864$ ,  $y = 0.4153$  is 2.39G 6.89/8.01.

The hue includes the initial of the color such as G for green and PB for purple-blue. The value indicates lightness or darkness; a color with a value of 9 is very light, while one with a value of 2.5 is nearly black. A high chroma such as 8 or 10 signifies a very pure color, and a low chroma of 1 or 2 shows a major component of gray. Strictly neutral grays are specified on the Munsell neutral value scale, which is not used in this report.

The spectra for colors other than green were treated in the same way. Where adjustment to a common film thickness was desired, the measured absorbance was corrected to an  $A_{\text{max}}$  of 2.00 for the initial green of that experimental film, using Equation 1.

### 3. Principal Colors

Constant colors observed over fairly wide potential ranges between the transitions are ascribed to different chemical forms, or oxidation states, of lutetium diphthalocyanine. These are designated as principal colors in this report. It should be noted that the principal color classification results from the electrochemical and spectroscopic behavior of the display material. It is not a human-factors classification. However, it happens that all of the principal colors are aesthetically pleasing. Some are of high purity, and the series affords versatile combinations for display purposes.

With chloride electrolytes, five principal colors were recognized in the pH range of 1 to 7: Orange, green, light blue, dark purple-blue, and violet. Table 4 summarizes experimental conditions for observation of these colors and lists the corresponding Munsell notations referred to a maximum absorbance of 2.00 for the initial green film. The cycled green showed the usual slight difference from the initial green. The orange, or yellow-red, of this series was not as red as the oxidation product observed previously with oxygen present. Two light blues, as well as two violets, were found, and the spectra changed significantly in both cases around pH 4.

TABLE 4

PRINCIPAL COLORS OF LUTETIUM DIPHthalOCYANINE FILM  
IN OXYGEN-FREE ELECTROLYTES CONTAINING CHLORIDE ION

A. EXPERIMENTAL DATA AND  $n$  VALUES<sup>a</sup>

Appearance	Typical Cell Conditions		$\lambda_{\max}$ (nm)	$n$ Relative to Cycled Green
	pH	Potential (V vs Ag/AgCl)		
Green (Initial) <sup>b</sup>	--	--	665	--
Orange	7.2	1.00	695,492	1
Green (Cycled)	7.2	0.10	661	0
Light Blue	7.2	-0.80	629	1
pH >4	~1	-0.20	650	1
pH <4	1.3	-0.35	559	3
Dark Purple-Blue				
Violet	7.2	-1.10	510	2
pH >4	~1	-0.50	564,478	Not determined
pH <4				

B. COLOR NOTATIONS WITH  $A_{\max} = 2.00$  FOR INITIAL GREEN

Appearance	CIE			Munsell	
	Y	x	y	Hue	Value/Chroma
Green (Initial)	0.416	0.286	0.415	2.4 G	6.9/8.0
Orange	0.403	0.397	0.358	3.8 YR	6.8/5.2
Green (Cycled)	0.497	0.270	0.433	3.2 G	7.4/10.5
Light Blue	0.292	0.205	0.278	2.5 B	5.9/8.1
pH >4	0.534	0.205	0.307	8.9 BG	7.7/10.7
pH <4	0.111	0.257	0.262	4.1 PB	3.9/3.5
Dark Purple-Blue					
Violet	0.142	0.318	0.251	9.1 P	4.3/5.8
pH >4	0.220	0.302	0.270	6.0 P	5.2/4.3
pH <4					

<sup>a</sup>The numbers of electrons ( $n$ ) in the various electrochromic reactions are discussed in Sections III-B and III-C. Orange product was formed by loss of electrons; others were formed by gain of electrons.

<sup>b</sup>Initial green dye film, as deposited, before placing the electrochemical cell.

## B. pH-POTENTIAL-COLOR RELATIONSHIPS

Figure 5 correlates the principal colors of the dye with pH and potential. The experimental points defining the color boundaries represent mid-points of the spectral transitions. These potentials were identifiable to about  $\pm 0.05$  V because abrupt changes in the shapes of the spectra occurred on either side of the transition. An example of a mid-point spectrum is the intermediate curve at 0.55 V in Figure 2, where the major peaks for green and orange are almost equally prominent.

### 1. Pourbaix Diagrams

Figure 5 is a type of chart known in electrochemistry as a Pourbaix diagram,<sup>(20)</sup> after Marcel Pourbaix, who made an extensive compilation of such data for elements throughout the Periodic Table. The diagram is precisely applicable only to systems at equilibrium, where the net current is zero. However, in many cases, it is a practical guide to behavior of an electrode under current flow. The Pourbaix diagram is based on the following principles:

Many electrode reactions in water utilize hydrogen ions and can be represented by



where Ox and Rd are the oxidized and reduced chemical species comprising the electrochemical couple. The equilibrium electrode potential  $E_{\text{eq}}$  is given by the Nernst equation

$$E_{\text{eq}} = E^\circ + (RT/nF) \ln(a_{\text{Ox}} a_{\text{H}}^n / a_{\text{Rd}}) \quad (3)$$

in which  $E^\circ$  is a standard potential on the selected electrochemical reference scale, the  $a$ 's are activities (effective concentrations) of the respective species,  $R$  is the gas constant,  $T$  is the absolute temperature, and  $F$  is the value of the faraday, or charge required to convert one gram-equivalent weight of a reacting material.

For the special case where  $a_{\text{Ox}} = a_{\text{Rd}}$ , Equation 3 takes the form

$$E_{\text{eq}} = E^\circ + (RT/F) \ln a_{\text{H}}^+ \quad (4)$$

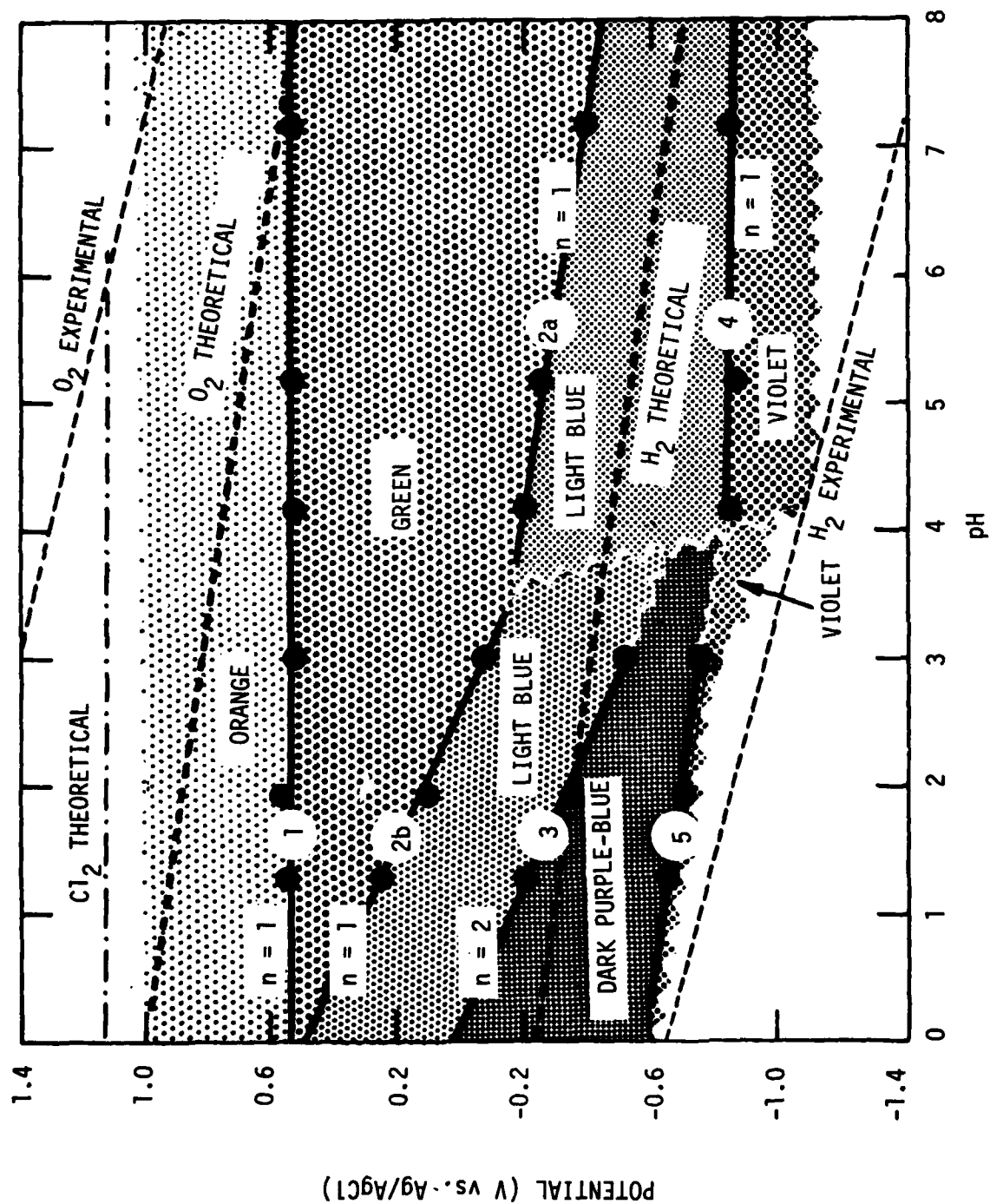


Figure 5. pH-Potential-Color Diagram

Since the pH is defined by

$$\text{pH} = -\log_{10} a_{\text{H}^+} \quad (5)$$

the potential may be expressed, at 25°C, by

$$E_{\text{eq}} = E^\circ - 0.0591(\text{pH}) \quad (6)$$

This very simple form describes many of the lines found in Pourbaix diagrams. A slope of -59 mV per unit of pH implies that equal numbers of hydrogen ions and electrons are used in the reaction. This is a common occurrence, especially with organic systems. Other slopes indicate chemical processes different from Reaction I. Above a pH-potential line, the electrochemical couple exists essentially all in the Ox form; below the line, it exists as Rd.

## 2. The Lutetium Diphthalocyanine Diagram

The lutetium diphthalocyanine system includes several of these couples, which are conveniently designated as orange/green, green/light blue, and so forth. Since the spectral transition points corresponded closely to the condition  $a_{\text{ox}} = a_{\text{rd}}$ , and the external current was nearly zero, it is appropriate to treat Figure 5 as a Pourbaix diagram. Few data were obtained on the dye system beyond the upper and lower sawtooth edges of the shaded area. Other sawtooth edges denote color-zone borders that are not yet well defined experimentally.

In addition to the dye plots, the chart includes broken lines representing the thermodynamic decomposition of water to hydrogen and oxygen. This inner pair of broken lines indicates the potentials vs Ag/AgCl at which water would be electrolyzed to produce those gases on metallic electrodes with zero overvoltage. The total cell voltage for the electrolysis of water is, theoretically, 1.23 V, independent of the pH. This is the distance between the inner broken lines. The thermodynamic potential for chlorine evolution is the horizontal line at 1.14 V.

On a semiconductor electrode such as tin oxide, the useful working range of an inert electrolyte is generally greater than the thermodynamic

lines would indicate, because the electron energy levels of the semiconductor do not match the electron exchange levels of the water system. The working limits for bare tin oxide exposed to the electrolyte are given approximately in Figure 5 by the outer broken lines. These represent the experimental decomposition potentials measured on blank electrodes without the dye film.

### 3. Implications for Display Performance

With this background, much information on the display system can be derived from Figure 5. It is apparent, for example, that the principal colors orange, green, and light blue occur throughout the pH range investigated, and that they are stable there within the thermodynamic stability range of water. The dark purple-blue phase was found, as expected, at relatively small negative potentials in the more acidic solutions. Below pH 2, this phase also extends into the stability zone of water. It offers very dark colors useful in high-contrast displays.

The violets lie between the theoretical and experimental lines for hydrogen evolution. For that reason, caution must be taken, in switching to violet, to minimize electrolytic formation of hydrogen, which could dislodge the film from the substrate. The switching pulse should not be too negative or of too long duration.

The minimum voltages required to switch between the various colors may be read directly from the figure. Smaller pulses are needed at lower pH. For example, a light blue film should be switchable to orange with a potential step of about 0.5 V at pH 2, while the same color change requires a step of 1.1 V at pH 7. On this basis, use of the more acidic solution could save nearly 50% of the switching energy. The actual switching potentials will be somewhat larger than those predicted from Figure 5 because ohmic and electrochemical resistances must be overcome under current flow.<sup>(9)</sup> The ohmic term can be minimized by appropriate cell design.

The spectrum of the orange film was essentially constant from pH 1 to 7 with 1 M KCl present. Minor variations were found in the height of the principal absorption peak at 695 nm, as indicated in Figure 6. From

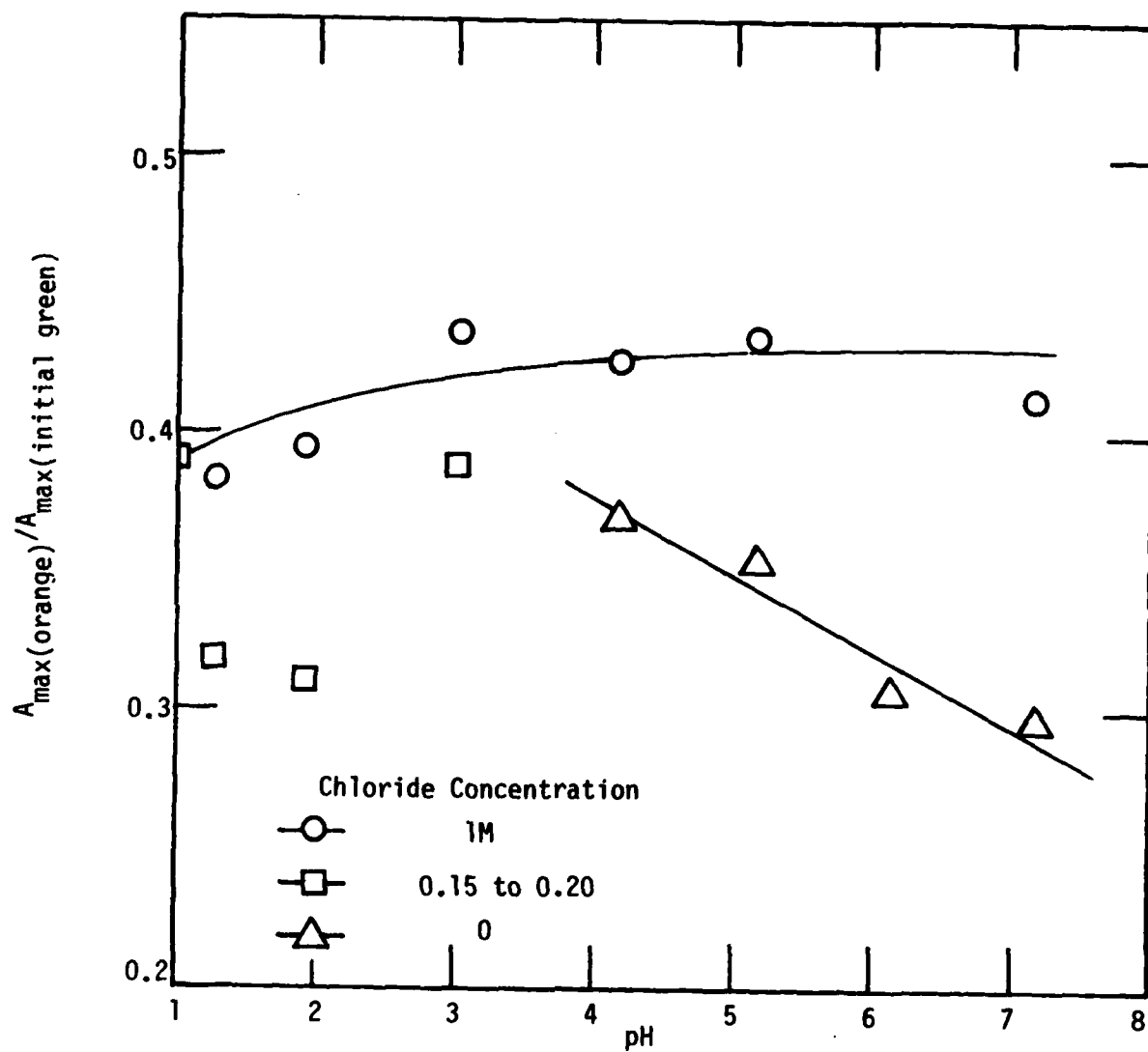


Figure 6. Dependence of Orange-Film Absorption-Peak Height on pH

the few points determined with chloride-free buffers containing phthalate and phosphate anions, the peak height appeared to increase with decreasing pH. In Figure 7, the spectrum of briefly cycled green films showed greater peak-height dependences on pH, but the other spectral characteristics were essentially unchanged.

#### 4. Fundamental Interpretations

The slopes of the lines in Figure 5 provide fundamental information on the color states. Line 1, for the orange/green transition, has a slope of zero. This was expected, since oxidation of the dye is known to proceed by the gain of anions, rather than the loss of protons.<sup>(4,7)</sup>

Line 2a, for the green/light blue process at  $\text{pH} > 4$ , has the slope of  $-68 \text{ mV}$ , which is close to that of  $-59 \text{ mV}$  in Equation 6. However, at lower pH, the segment labelled 2b has the rather surprising slope of  $-180 \text{ mV}$ . Apparently three protons were added for each electron transferred to the dye. This could occur by formation of an addition compound with two molecules of  $\text{HCl}$ . In fact, Figure 8 offers spectroscopic evidence of two light blue forms with different chemical compositions. The light blue in the more acidic solutions has a single peak at  $650 \text{ nm}$ , while the light blue at  $\text{pH} 7$  has a prominent peak at  $629 \text{ nm}$  and a lesser one at  $710 \text{ nm}$ .

Line 3 also has a slope of  $-175 \text{ mV}$ , suggesting addition of more  $\text{HCl}$ . Acid adducts are proposed here to account for the slopes in the Pourbaix diagram. These solid reaction products should be investigated further by chemical analysis to determine how much acid they actually contain. Spectra representative of those found between Lines 3 and 5 of the Pourbaix chart are shown in Figure 9. Curves (a) and (e) were recorded in  $0.1 \text{ M Cl}^-$ , and the others were obtained at lower chloride levels. A substantial component of light blue is seen in (d) and (e), while (a), (b), and (c) are thought to be those of the fully converted dark purple-blue form.

In contrast to Lines 2 and 3 in the Pourbaix diagram, Line 4 has zero slope. This does not imply that the corresponding light blue and violet films contain no hydrogen ions. It indicates that electrons transferring across Line 4 are compensated by metal cations such as  $\text{K}^+$  instead of additional  $\text{H}^+$ .

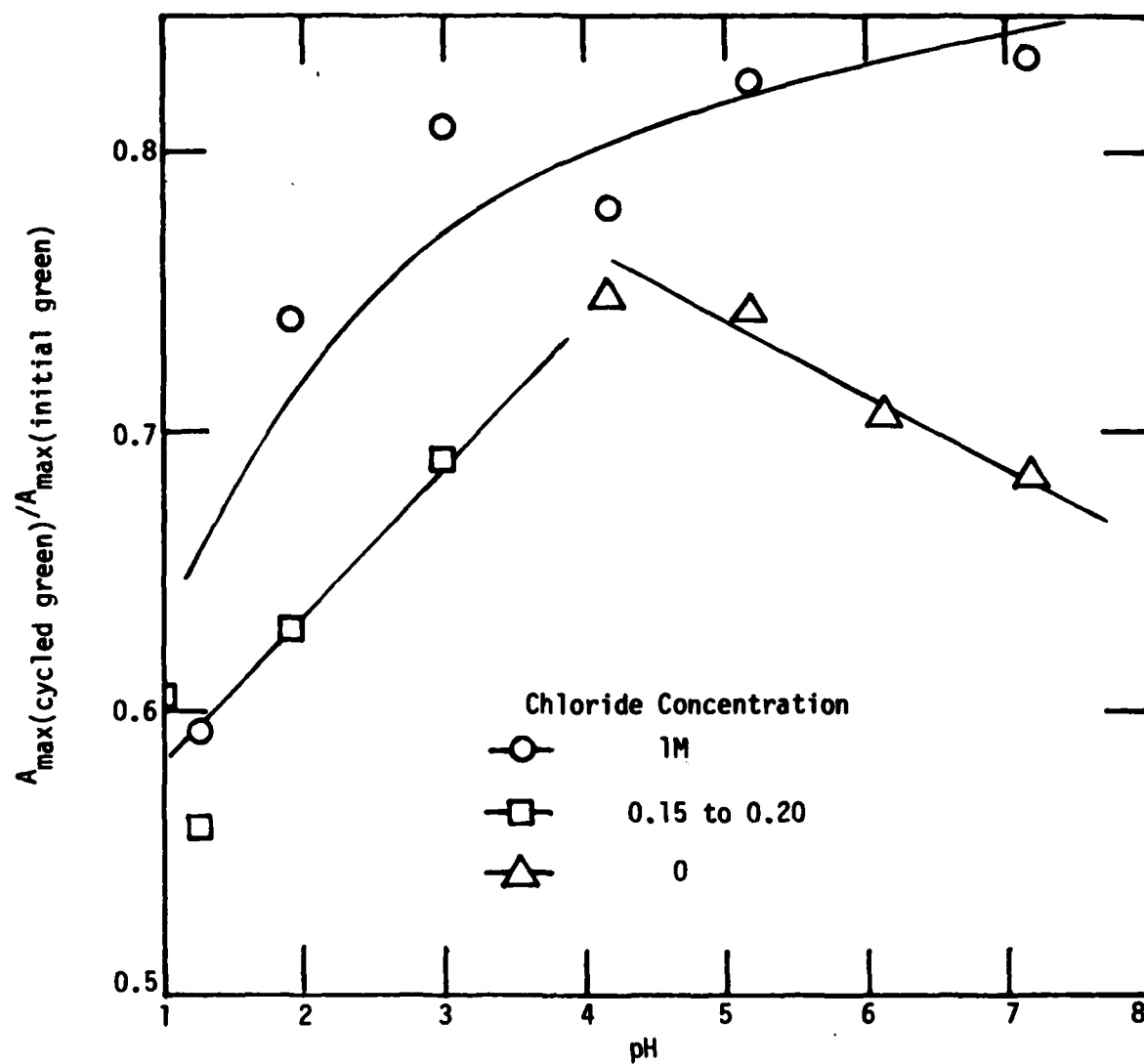


Figure 7. Dependence of Cycled-Green Absorption-Peak Height on pH

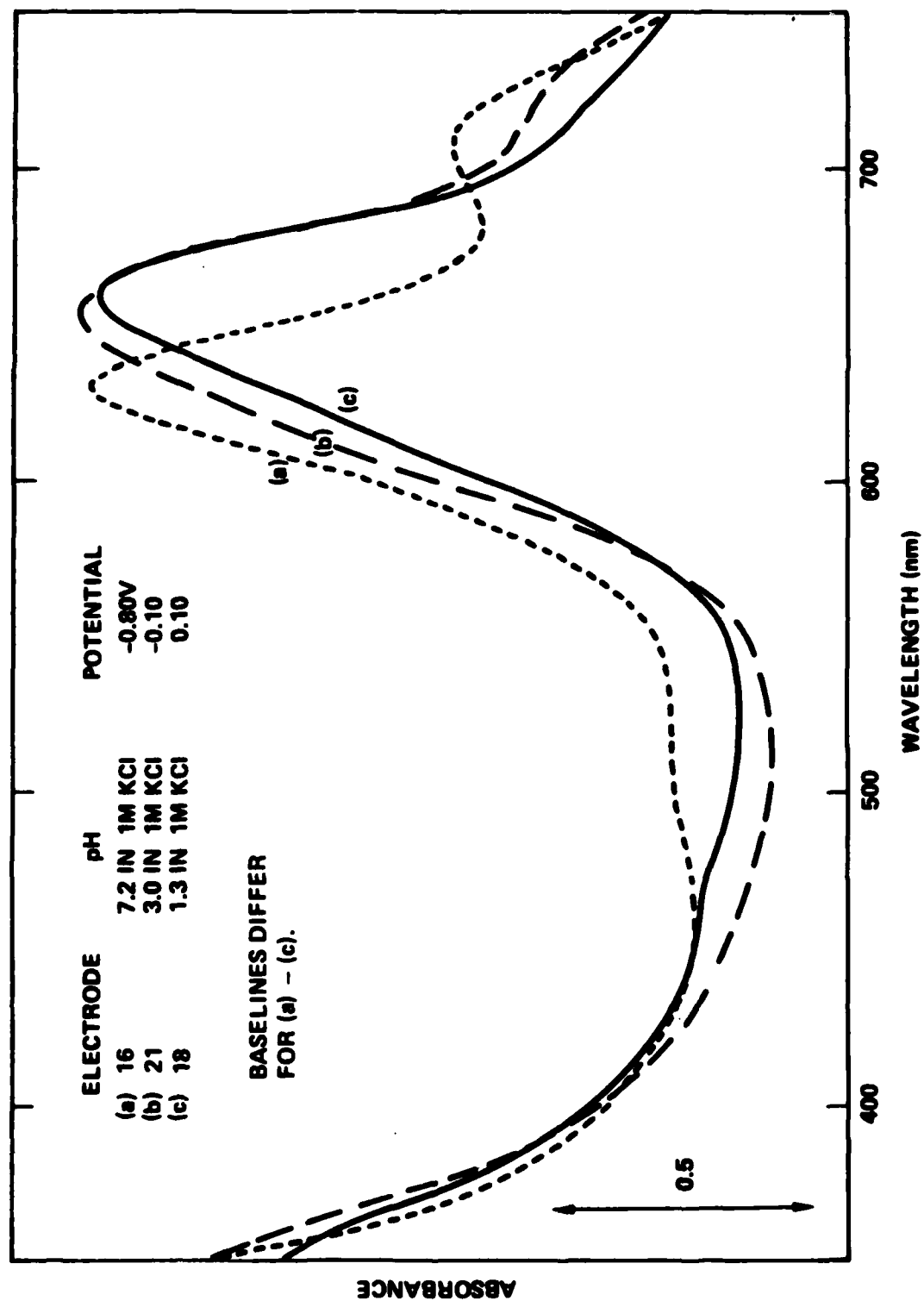


Figure 8. Spectra of Light Blue Films at Different pH Values

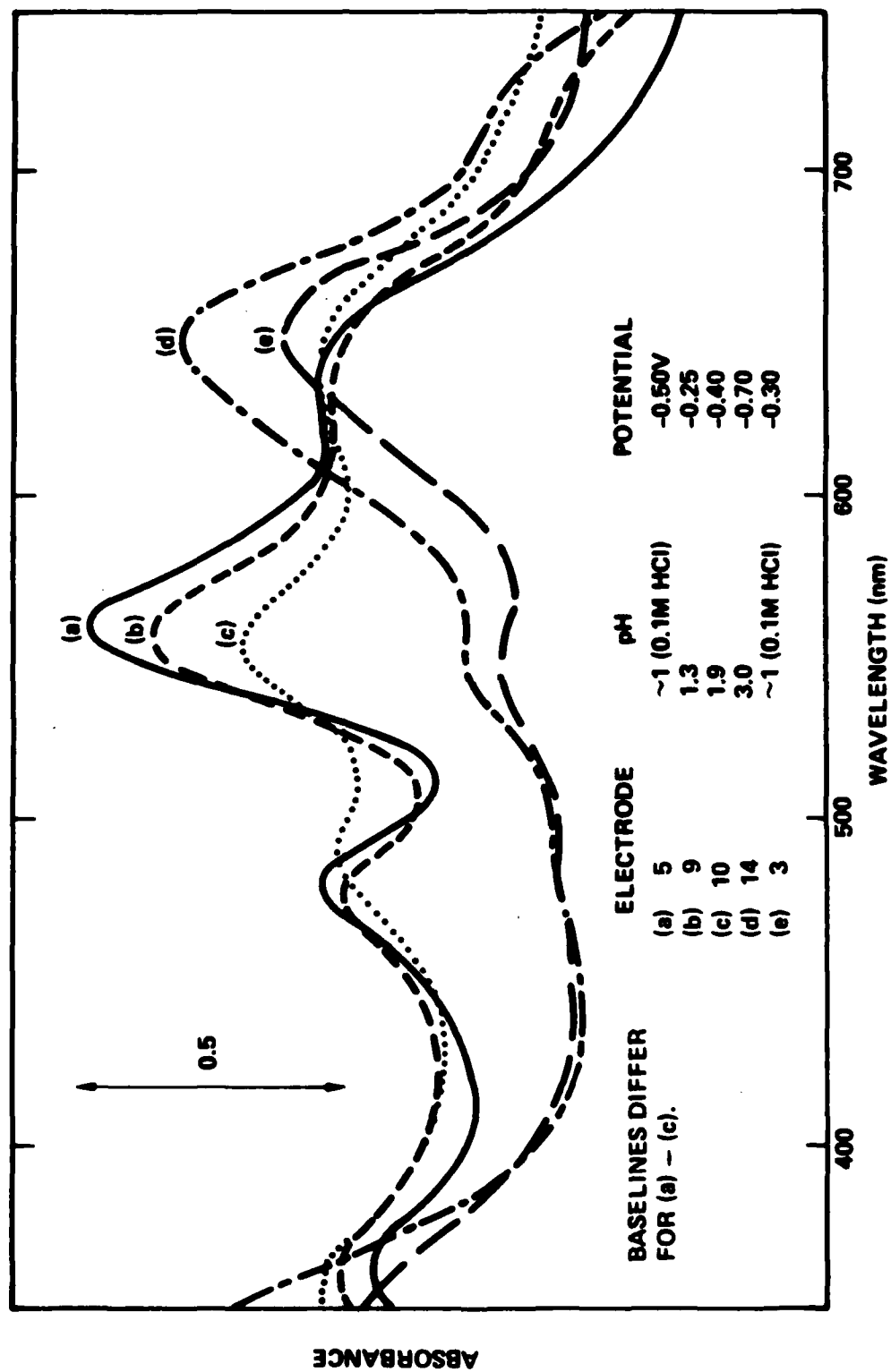


Figure 9. Spectra Observed within Dark Purple-Blue Region of pH - Potential Diagram

Along Line 5, data were difficult to obtain because the film tended to peel away from the substrate. Moreover, the violet below this line differed spectrally from that at  $\text{pH} > 4$ . This difference is seen by comparing Curve (d) of Figure 10, for violet at  $\text{pH} 1$ , with Curve (a) of the same figure for violet at  $\text{pH} 7$ . Curve (d) appears to be a flattened version of the spectra for dark purple-blue in Figure 9. If allowance is made for the peeling tendency (Section III-D-2), this resemblance suggests that the violet at  $\text{pH} < 4$  may be chemically the same as the dark purple-blue above it. If so, Line 5 probably represents hydrogen formation instead of a dye reaction.

When extrapolated, Lines 1 and 2b intersect near  $\text{pH} 0$ . At this point, the usual green should disappear, leaving as principal colors orange, blue-green (10BG 8/11), and purple-blue.

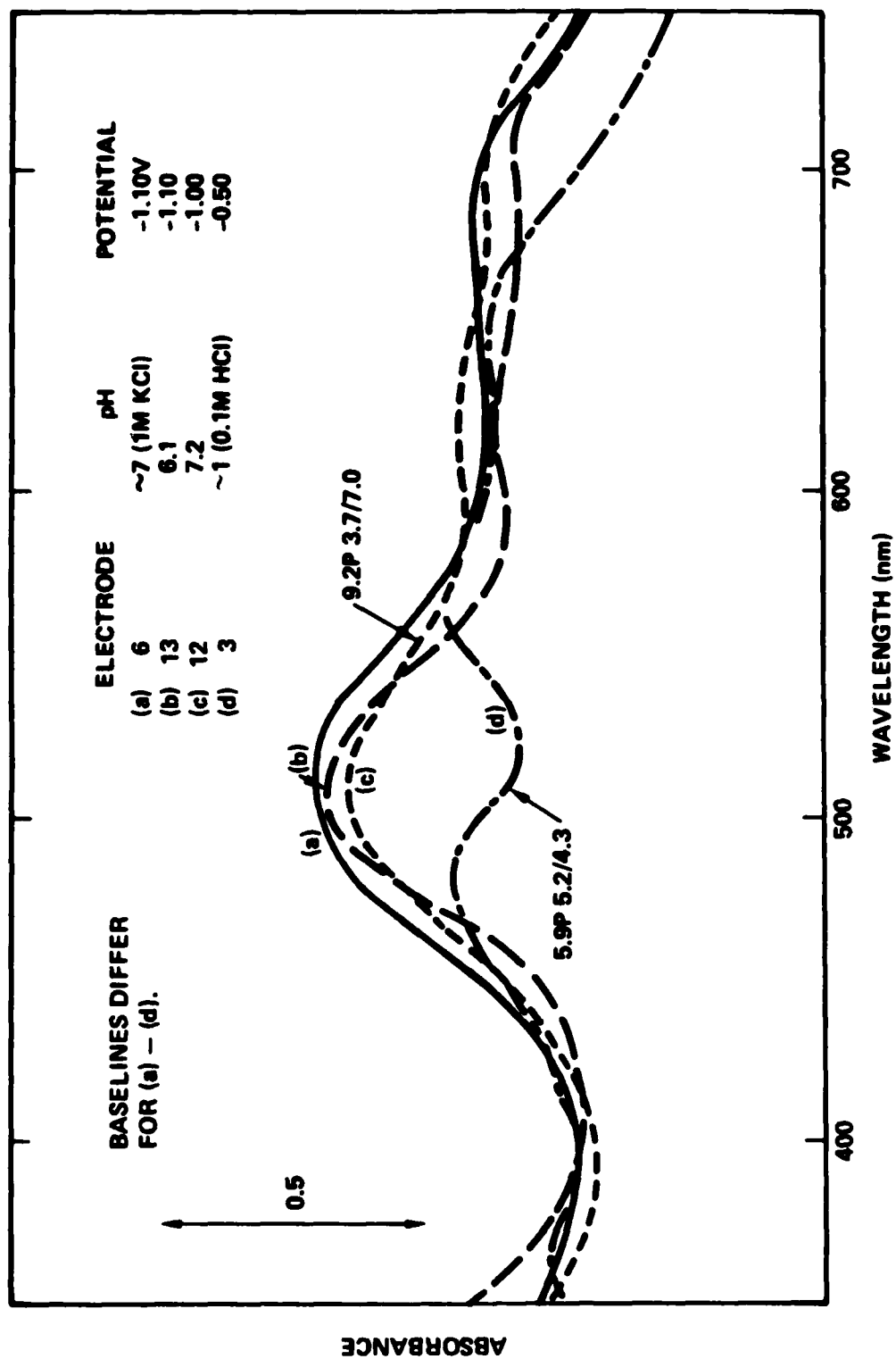


Figure 10. Comparison of Spectra for Violet Films at pH > 4 and pH < 4

## C. ELECTROCHEMICAL REACTIONS

### 1. n Values and Chemical Equations

Also noted on Figure 5, but not yet discussed, are the numbers ( $n$ ) of electrons per molecule of dye involved in the various color transitions. Figure 11 illustrates the method by which they were determined, using the incremental voltage-step technique. The total switching charge was obtained by adding the charges represented by the shaded rectangles. Since the number of molecules in the dye film was known from its optical density in the initial green state, the value of  $n$  was easily found. The upper broken line in Figure 11 approximates the curve that would be observed as the magnitude of the voltage increment approached zero. Adjacent processes were resolved as indicated by the coarser dashed lines.

The  $n$  values found in 1 M KCl and 0.1 M HCl are given in Table 5. One-electron processes were observed for all transitions except the light blue/dark purple-blue reaction in 0.1 M HCl. In that case, the apparent  $n$  varied with the voltage increment  $\Delta E$  that was used to measure it. The extrapolation to  $\Delta E = 0$ , in Figure 12, yielded a value close to 2.

The complexity of the lutetium diphthalocyanine electrochemical system is recognized in a 1982 review article from this laboratory.<sup>(15)</sup> It is possible, for example, that the green dye can exist as  $\text{LuPc}_2$  as well as  $\text{LuHPc}_2$ , and that it may interact reversibly with oxygen and water.\* A full discussion of such details is outside the scope of this report. It is appropriate, nevertheless, to write a reaction scheme suggested by the pH-potential-color relationships and  $n$  values found here and to compare it with previous results obtained by other experimental methods.

For convenience, the symbol  $D$  can represent a molecule of cycled green dye, i.e., a molecule that has been converted at least once to another color and returned to the green state. With that notation, the following equations can be proposed for the transitions at the lines of the Pourbaix diagram in Figure 5:

\*The phthalocyanine anion with the empirical formula  $\text{C}_{32}\text{H}_{16}\text{N}_8^-$  is often abbreviated  $\text{Pc}^-$ . Metal-free phthalocyanine is then represented by  $\text{H}_2\text{Pc}$ , and the lutetium(III) complex by  $\text{LuHPc}_2$ .

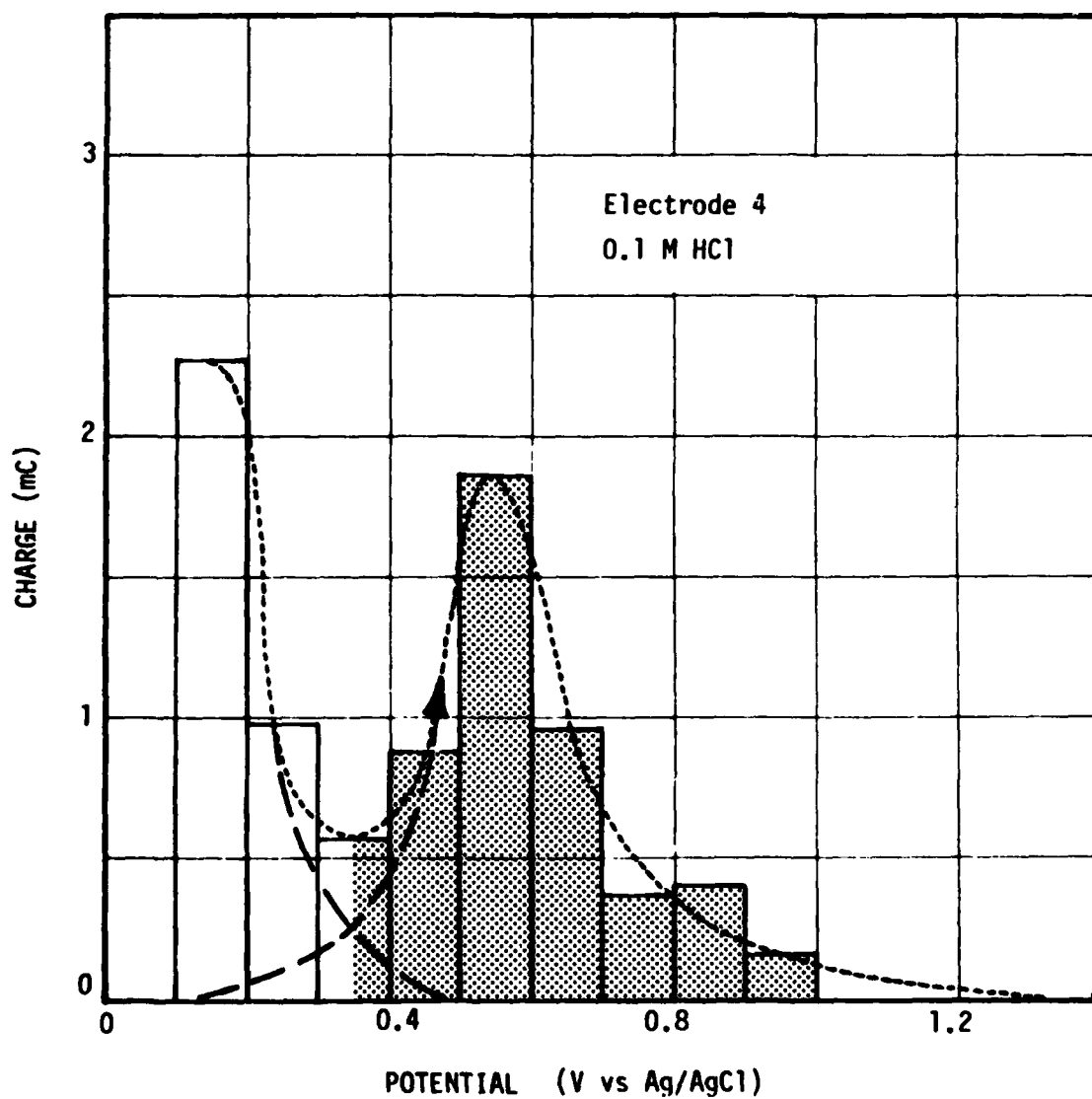


Figure 11. Determination of Switching Charge for Green-to-Orange Transition by Incremental Voltage Steps

TABLE 5

FARADAIC  $n$  VALUES FOR ELECTROCHROMIC TRANSITIONS OF LUTETIUM DIPHthalOCYANINE<sup>a</sup>

Electrolyte	Electrode	$\Delta E$ (V)	$n$ (Electrons per Molecule of Dye)					
			O $\rightarrow$ G	O $\rightarrow$ G	G $\rightarrow$ B	G $\rightarrow$ B	B $\rightarrow$ V	B $\rightarrow$ V
1 M KCl	6	0.1	--	1.53	1.36	--	0.94	--
	2	0.05	0.89	--	0.82	--	$\sim 1.26$	--
0.1 M HCl	5	0.1	--	0.87	--	--	--	5.69
	4	0.1	--	0.92	1.17	--	--	4.28
	7	0.05	0.72	0.79	0.98	0.95	--	--
	1	0.05	0.90	--	1.01	--	--	3.48
	7	0.025	--	--	--	--	--	--
	7	0.01	--	--	--	--	--	2.62
Average	8	0.001	--	--	--	--	--	2.48
			0.95		1.05		1.10	2.1 <sup>b</sup>

<sup>a</sup>Reaction products are designated by initials of the colors: O for orange, G for cycled green, B for light blue, V for violet (pH 7), and pB for dark purple-blue.

<sup>b</sup>Extrapolated; see Figure 12.

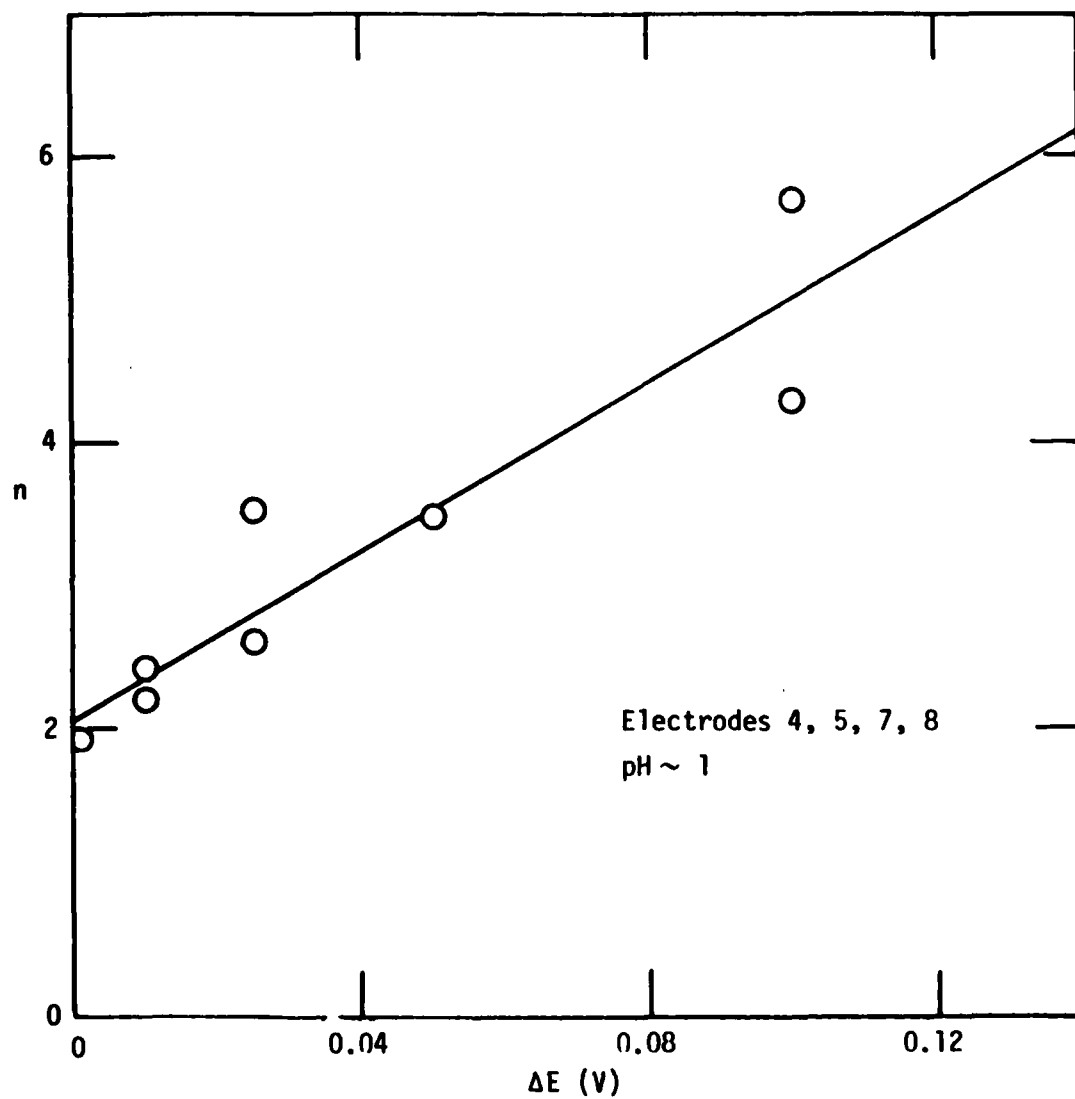
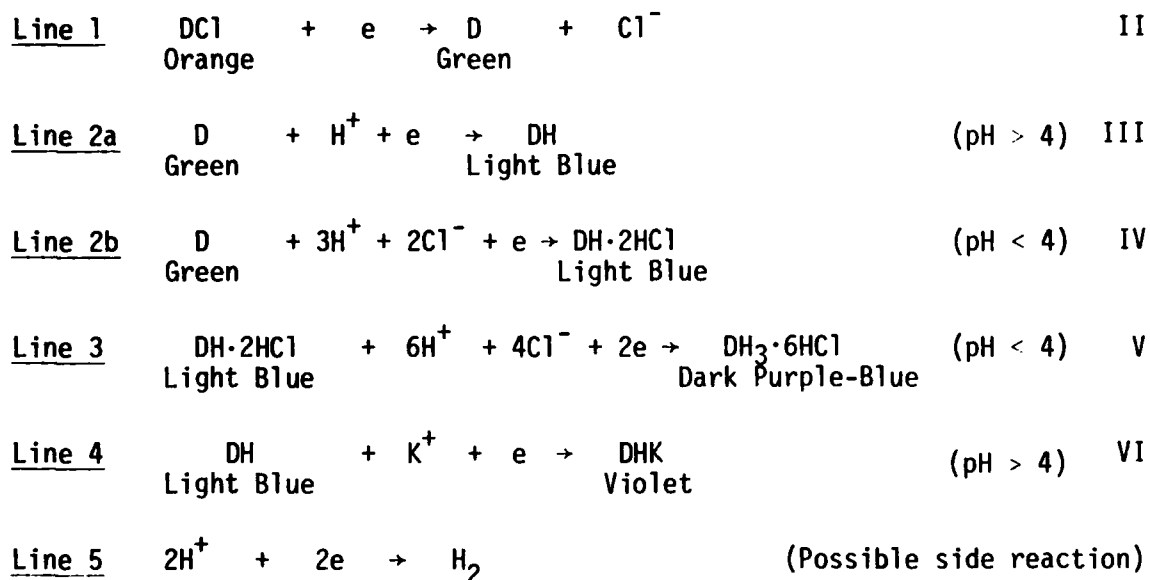


Figure 12. Dependence of Apparent  $n$  Value on Voltage Increment for the Light Blue/Dark Purple-Blue Transition in 0.1 M HCl



## 2. Comparisons with Previous Results

Orange and Red. The present study consistently produced an orange oxidation product with  $n = 1$  for the transition at 0.55 V vs Ag/AgCl. Previous experiments in neutral or slightly alkaline electrolytes under current flow have yielded brighter reds with  $n$ 's of about 2, although non-integral values often have been found.<sup>(4,6)</sup> Considerable evidence of oxygen sensitivity in the red mode also has been observed.<sup>(8,15)</sup> It now appears that oxygen--either ambient or electrolytically formed--may be involved in producing or sustaining the bright red color. There is no doubt that lutetium diphthalocyanine can form an excellent red. More work is needed, however, that color for display purposes.

Light Blue. An  $n$  value of 1 was found in green/light blue boundary-propagation experiments<sup>(11)</sup> with LiCl in nonaqueous solvents, where the only cation present was Li<sup>+</sup>. However, propagations in unbuffered aqueous KCl indicated  $n = 2$  and were presumed to occur with uptake of 2K<sup>+</sup>. It is possible that the pH dependence of the green/light blue transition would disappear in the Pourbaix chart at pH > 7, but where enough H<sup>+</sup> is available. It seems to be favored over K<sup>+</sup> as the compensating cation for the light blue product.

Dark Purple-Blue. An  $n$  value of 3.5 was estimated for propagation of this dark color in a green film contacted by 1.2 M HCl, but only by extrapolation of higher apparent  $n$ 's to zero applied current density.<sup>(11)</sup> An  $n$  value of 3 for  $G \rightarrow PB$  in that case corresponds exactly to the  $n$  of 2 determined here for  $R \rightarrow PB$  by extrapolation to  $\Delta E = 0$ . The need for extrapolation to zero-current conditions in both types of measurements indicates a side reaction, which very probably is hydrogen formation. The problem is not associated with tin oxide only, since no tin oxide was present in the boundary propagations. It could be a question of how fast HCl is assimilated by the dye. If the electrode is forced beyond such a limiting rate, the next available process will occur. The apparent  $n$  then is abnormally large, and damage can be done to the film if a gaseous product is formed.

#### D. MODIFIED COLORS

Brief inspection of Figure 5 might suggest that the dye can produce only principal colors identified with specific phases of the Pourbaix chart. This actually is not so. It is shown in Part 1, below, that many additional colors are available in continuous gradations through controlled blending of the principal colors. Still other color changes can result from discontinuities in the dye film. These are treated quantitatively in Part 2.

##### 1. Blended Colors

The blending of colors adds heightened optical contrast and aesthetic variety to the display. It is done by controlling the charge injected, so that the system stays in a transitional region. With a specified current-time input or a programmed cut-off at a predetermined charge level, the electrochemical reaction can be stopped before conversion is complete. The result is a mixed chemical system with predictable color characteristics.

The colors obtainable in this way from lutetium diphthalocyanine were determined by computer blending. It was assumed that the reactant and product forms of the dye were uniformly distributed over the film area--either as a molecular mixture or as two parallel layers, each of uniform thickness. Barring specific interactions of the molecules, these distributions should be visually indistinguishable. At any wavelength, the absorbance of the blend is given by

$$A_{\text{blend}} = (1 - p)A_1 + pA_2 \quad (7)$$

where  $A_1$  and  $A_2$  are the absorbances of the first and second principal colors, and  $p$  is the fraction of the dye molecules converted from the first to the second state. The complete absorption spectrum of the blend can be constructed in this way. For color computations, it is sufficient to know the blended absorbances at the wavelengths in the ten-selected-ordinate sets. The evaluation of CIE and Munsell coordinates then proceeds as in Table 3.

Results of such color blending in the orange/green, green/light blue, and light blue/violet transitional regions are given in Table 6 and Figures 13-15. All of these calculations were based on a maximum absorbance of 2.00 for the initial green film. Among the calculated Munsell

TABLE 6  
TRANSITIONAL COLORS IN THE LUTETIUM DIPHthalOCYANINE SYSTEM<sup>a</sup>

A. YELLOWISH BLENDS OF ORANGE AND GREEN (FIGURE 13)						
p	Appearance	CIE Notation			Munsell Notation	
		Y	x	y	Hue	Value/Chroma
0	Orange	0.403	0.397	0.358	3.8 YR	6.8/5.2
0.20	}	0.409	0.368	0.372	2.5 Y	6.9/3.4
0.24		Grayish Yellow	0.411	0.362	0.376	5.1 Y
0.40	}	0.421	0.341	0.386	5.0 GY	6.9/3.6
0.60		Yellow-Green	0.439	0.316	0.401	9.7 GY
0.80	}	0.464	0.293	0.416	2.0 G	7.2/7.9
1.00		Green	0.497	0.270	0.433	3.2 G

B. BLUE-GREEN BLENDS OF LIGHT BLUE (pH >4) AND GREEN (FIGURE 14)						
p	Appearance	CIE Notation			Munsell Notation	
		Y	x	y	Hue	Value/Chroma
0	}	0.497	0.270	0.433	3.2 G	7.4/10.5
0.20		Green	0.440	0.254	0.404	5.6 G
0.40	}	0.393	0.239	0.373	9.8 G	6.7/9.3
0.60		Blue-Green	0.354	0.226	0.341	4.0 BG
0.66	}	0.343	0.222	0.332	4.9 BG	6.4/8.5
0.80		Light Blue	0.320	0.215	0.309	8.1 BG
1.00		0.292	0.205	0.278	2.5 B	5.9/8.1

<sup>a</sup>Transitional colors are computer blends of principal colors included in Table 4. Absorbances were adjusted to  $A_{\max} = 2.00$  for initial green.

TABLE 6 (CONTINUED)

C. PURPLE-BLUE BLENDS OF LIGHT BLUE (pH >4) AND VIOLET<sup>b</sup> (pH >4) (FIGURE 15)

p	Appearance	CIE Notation			Munsell Notation	
		Y	x	y	Hue	Value/Chroma
0	} Light Blue	0.292	0.205	0.278	2.5 PB	5.9/8.1
0.20		0.219	0.221	0.261	7.2 B	5.2/6.5
0.30		0.191	0.230	0.253	0.4 PB	4.9/6.0
0.40	} Purple-Blue	0.169	0.240	0.247	3.6 PB	4.7/5.6
0.44		0.161	0.244	0.244	7.5 PB	4.4/5.5
0.60		0.135	0.262	0.237	9.1 PB	4.2/5.5
0.80	} Violet	0.114	0.288	0.231	4.8 P	3.9/6.1
1.00		0.101	0.320	0.232	9.2 P	3.7/7.0

<sup>b</sup>Corrected for 6% spalling (Section III-D-2)

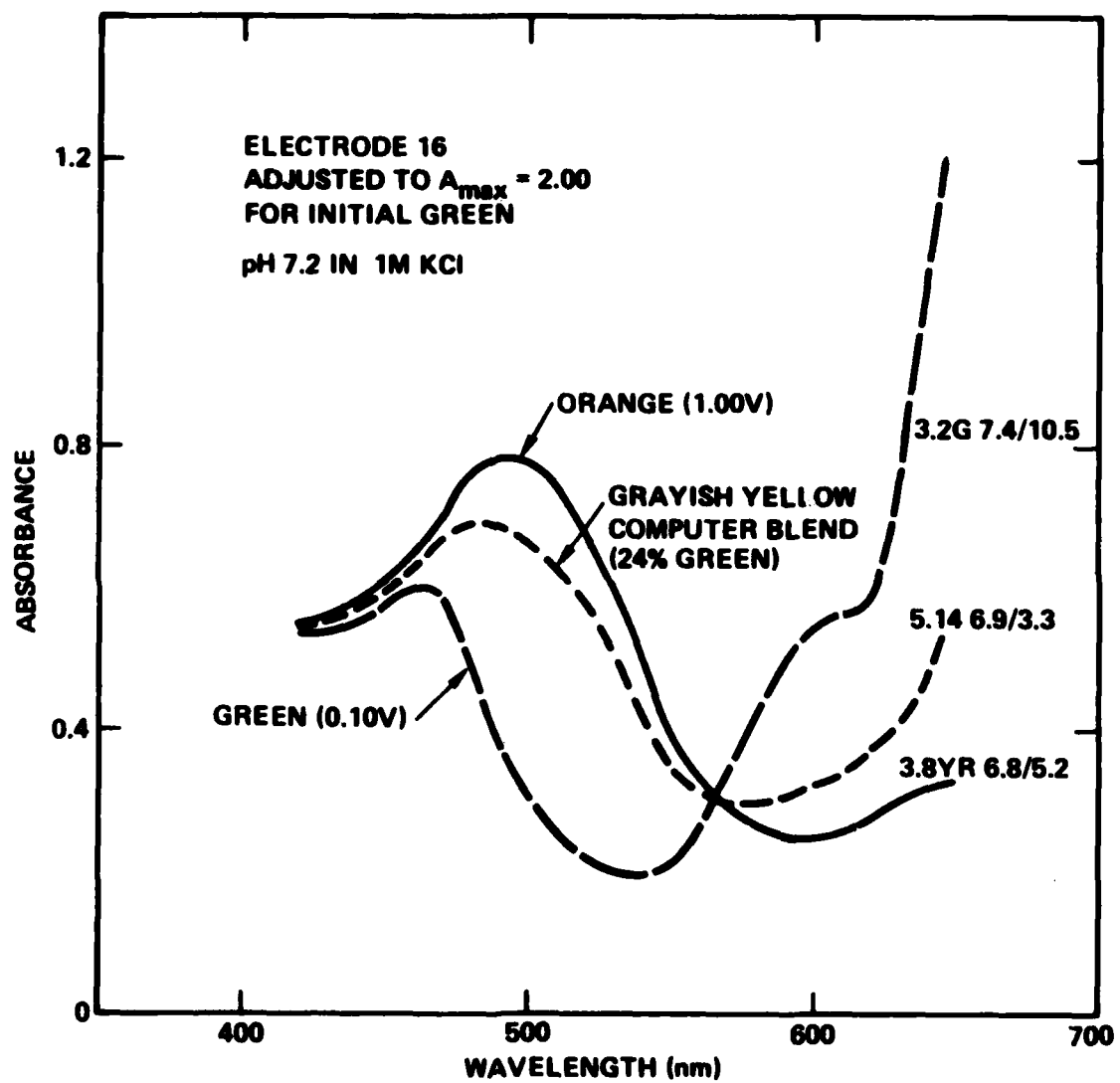


Figure 13. Computer Blending of Orange and Green to Grayish Yellow

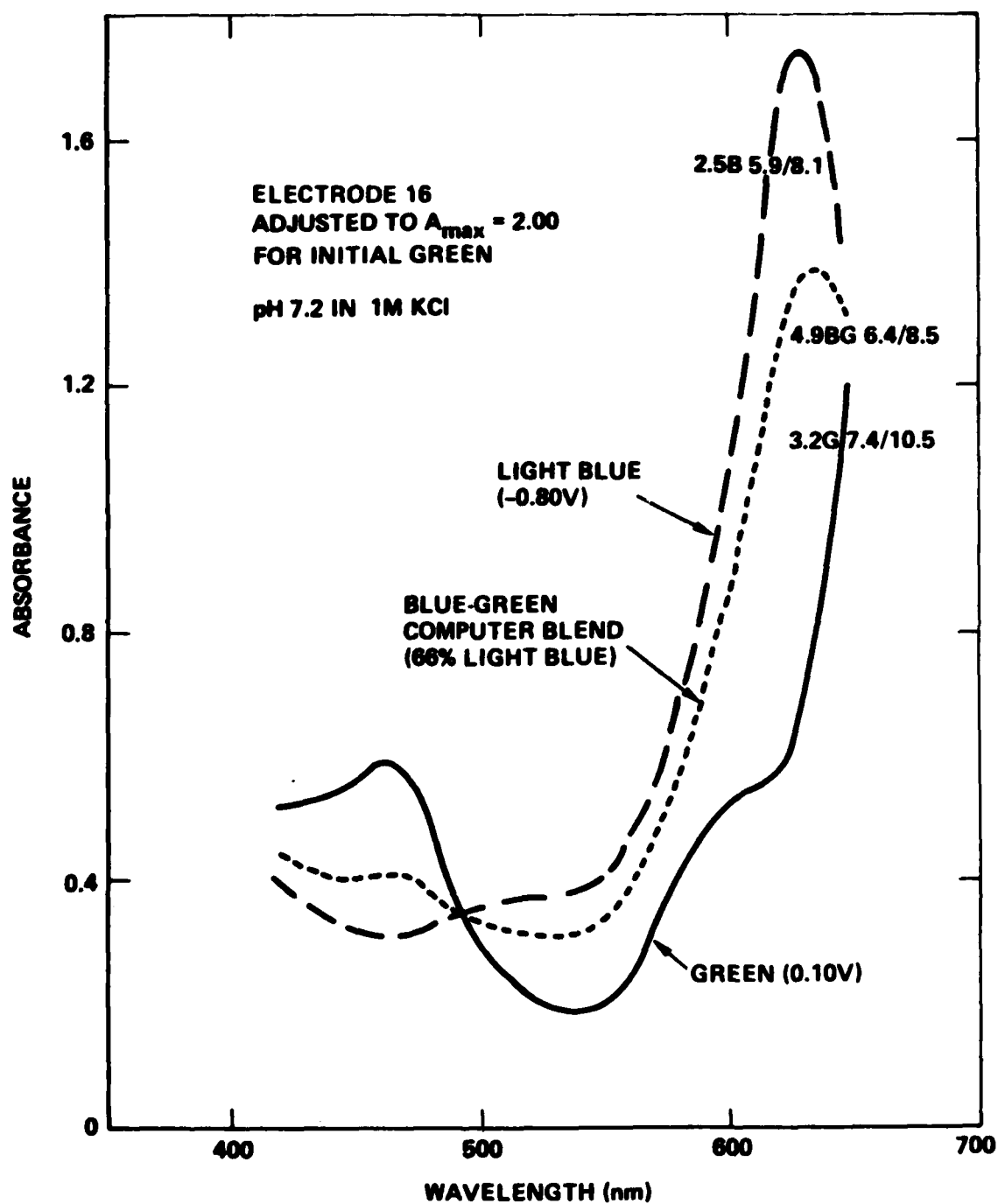


Figure 14. Computer Blending of Green and Light Blue to Blue-Green

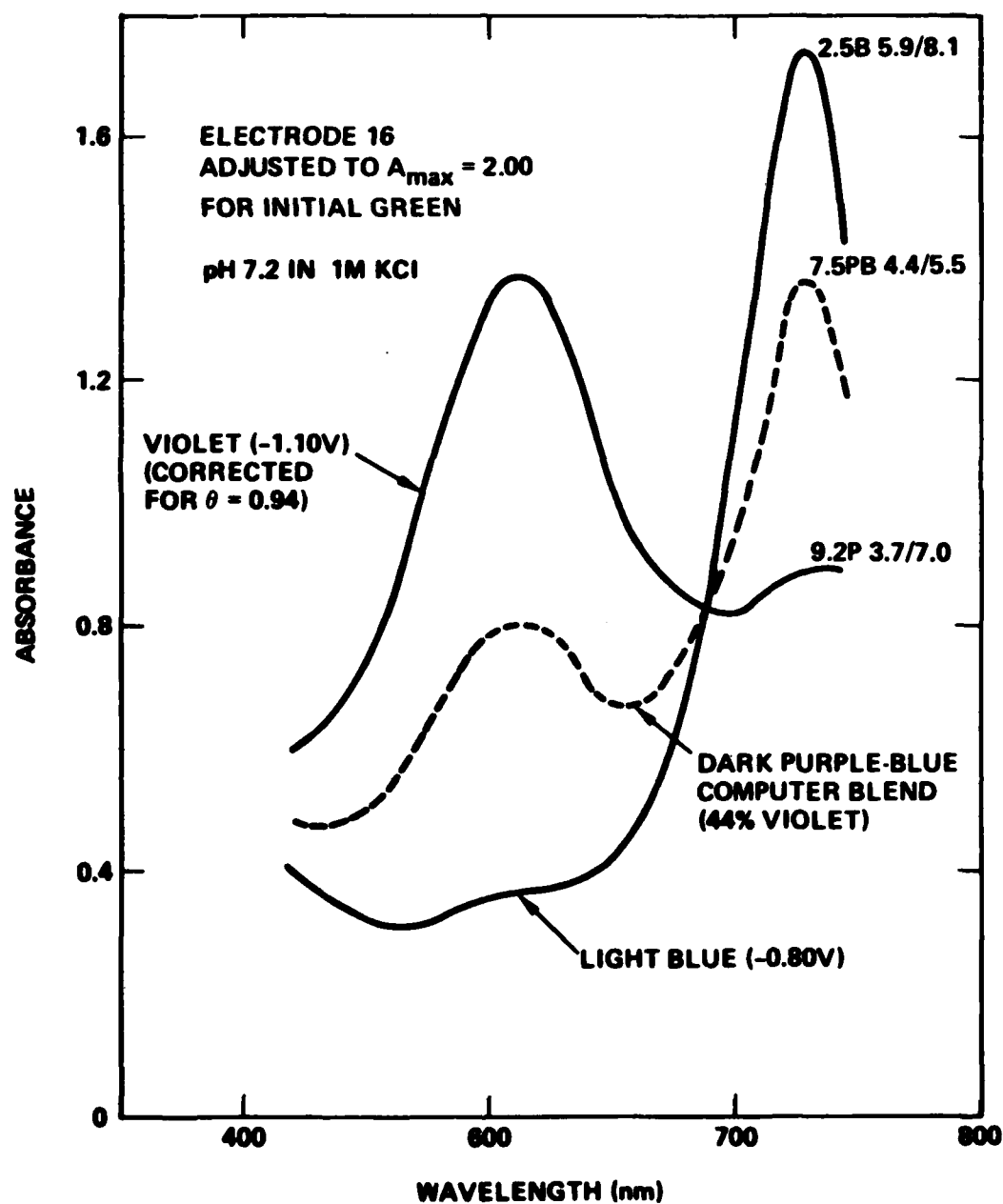


Figure 15. Computer Blending of Light Blue and Violet to Dark Purple-Blue

colors were those often seen in transitory states of model cells. With the p, or charge, specifications available, such colors now should be producible at will.

Yellows. In an earlier paper, it was suggested that the yellow form of lutetium diphthalocyanine might be a 1-electron oxidation product.<sup>(15)</sup> It is now apparent from the charge measurements and spectra that the yellow material is a mixture, rather than a discrete reaction product. The purest yellow identified in this study was 5.1Y 6.9/3.3 (nearest Munsell chip 5Y 7/4), for a film consisting of 24% green and 76% orange. With the spectrum shown in Figure 13, this yellow has a grayish cast. An ideal, visually pure yellow is perceived with monochromatic light at 580 nm. It is evident that the absorption of the yellow blend is still substantial at this wavelength, although it rises fairly symmetrically on either side of 580. A subtle difference in one of the contributing spectra could have a pronounced effect on the blended color in this case. Such differences may exist among the many rare-earth diphthalocyanine-electrolyte combinations still to be investigated; hence, a more saturated yellow is not ruled out. In any event, the yellow obtained here offers high contrast with blue, green, and purple-blue or violet.

Blue-Greens. The blue-greens of Figure 14 and Table 6 (B) are exceptionally pure and pleasing colors that occur at easily accessible potentials. They should be quite satisfactory for brightly colored information displays.

Alternative Dark Blue. An interesting result, not anticipated visually from the principal colors, occurred on blending light blue and violet at pH > 4. A deep blue, 7.5PB 4.4/5.5, was found at 44% violet. Its spectrum is given in Figure 15. For many display purposes, this blend could be used in place of the principal color 4.1PB 3.9/3.5, which was found under conditions where hydrogen formation appeared to be a greater problem (Section III-B-4).

## 2. Discontinuous Films

Cycled films of lutetium diphthalocyanine eventually lose color intensity and purity. Under very adverse conditions, such as hydrogen

evolution, this can occur on the first cycle or soon thereafter, with obvious peeling of the dye from the substrate. More limited cracking could also result from phase changes, even with an electrode of long cycle life. Hence, it was of special interest to examine the effect of film discontinuities on color.

#### a. Models

Two models considered for this purpose are illustrated by Figure 16. The symbol  $\theta$  represents the fraction of the substrate surface covered by the dye film. In the stacking model, the dye detached from certain areas is assumed to be uniformly distributed on top of the remaining film. In the spalling model, the detached dye is lost completely and no longer in the light path.

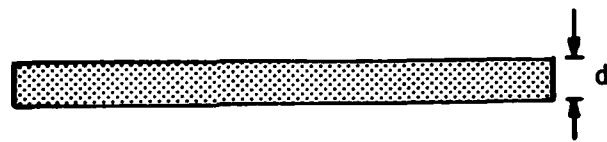
The stacking model is equivalent to a model for light absorption by inhomogeneous samples in spectrophotometry which was described by Jones in 1952.<sup>(21)</sup> It was recognized in that case that all of the absorbing material, if aggregated in a fraction  $\theta$  of the light-beam area, would have a concentration  $c/\theta$ , where  $c$  represented the average concentration of the sample. In the stacking model of the dye film, the thickness is increased in the light-absorbing areas by the factor  $1/\theta$ . Then, from Jones' result, the observed absorbance  $A_{\text{obs}}$  of the discontinuous film should be related to the true absorbance  $A_{\text{true}}$  of the initial film by Equation 8.

$$A_{\text{obs}} = -\log[\theta 10^{-A_{\text{true}}/\theta} + (1-\theta)] \quad (\text{Stacking}) \quad (8)$$

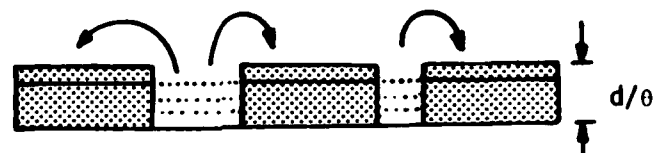
For the spalling model, the absorbance in the covered areas remains unchanged, and the observed absorbance is given by

$$A_{\text{obs}} = -\log[\theta 10^{-A_{\text{true}}} + (1-\theta)] \quad (\text{Spalling}) \quad (9)$$

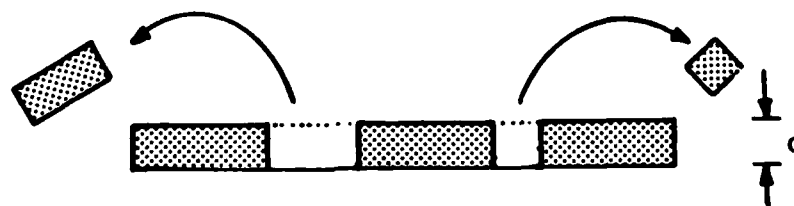
It is assumed for both models that the discontinuities in the film are considerably greater than the wavelength of the light, so that diffraction is negligible, and smaller than the resolution limit of the detector, so that the film as a whole appears uniform. Light scattering is also neglected.



(a) Original Continuous Film ( $\theta=1$ )



(b) Stacking Model ( $\theta=0.75$ )



(c) Spalling Model ( $\theta=0.75$ )

Figure 16. Models for Discontinuous Films with 75 Percent Surface Coverage

Equations 8 and 9 provide the means for predicting changes in the observed spectrum due to discontinuities because  $A_{\text{true}}$  is wavelength-dependent. It is apparent in Figure 17 that the effect of discontinuity is relatively greater at high absorbance than at lower absorbance; discontinuity flattens the spectrum. Plots of  $A_{\text{obs}}$  vs  $A_{\text{true}}$  are given for both models at several values of the fractional coverage  $\theta$ . The calculated curves are very similar at  $\theta = 0.99$  but diverge significantly at  $\theta = 0.80$ .

b. Application to Experimental Cases

The experimental points in Figure 17 are for a green film, taking  $A_{\text{true}}$  from the spectrum of the initial green. With  $\theta = 0.93$  to  $0.94$ , either model fits the data rather well. The spalling model seems more realistic physically, since uniform splitting and stacking of the dislodged particles is improbable.

Assessment of Film Damage. Figure 18 illustrates application of the spalling model to the spectrum of a green film that may have been damaged by cycling to violet. With an assumed surface coverage of  $0.936$ , Curve (c) was converted, through Equation 9, to Curve (d), which closely approximates the experimental spectrum (b) of a green film that was cycled only once to orange. The differences between (a) and (b) are typical of early-stage orange/green cycling in a chloride electrolyte.\*

Prediction of Brighter Colors. The orange and red colors obtained with lutetium diphthalocyanine often are not as vivid as desired. Bright reds can be formed, however, as noted in Section III-C-2. The possibility of predicting a bright red by correcting an orange-film spectrum with the spalling model was examined. The results are shown in Figure 19. A favorable trend was found with the assumption of lower coverages for the experimental film, but the corrected color for  $\theta = 0.85$  still fell among the orange or yellow-red hues rather than the reds. Thus, the differences between the orange and red are not explained by cracking of the film.

\*Some of those differences could be due to chemical effects such as hydration of the film, since the cycled film had higher absorption than the original in the 470 to 570-nm region.

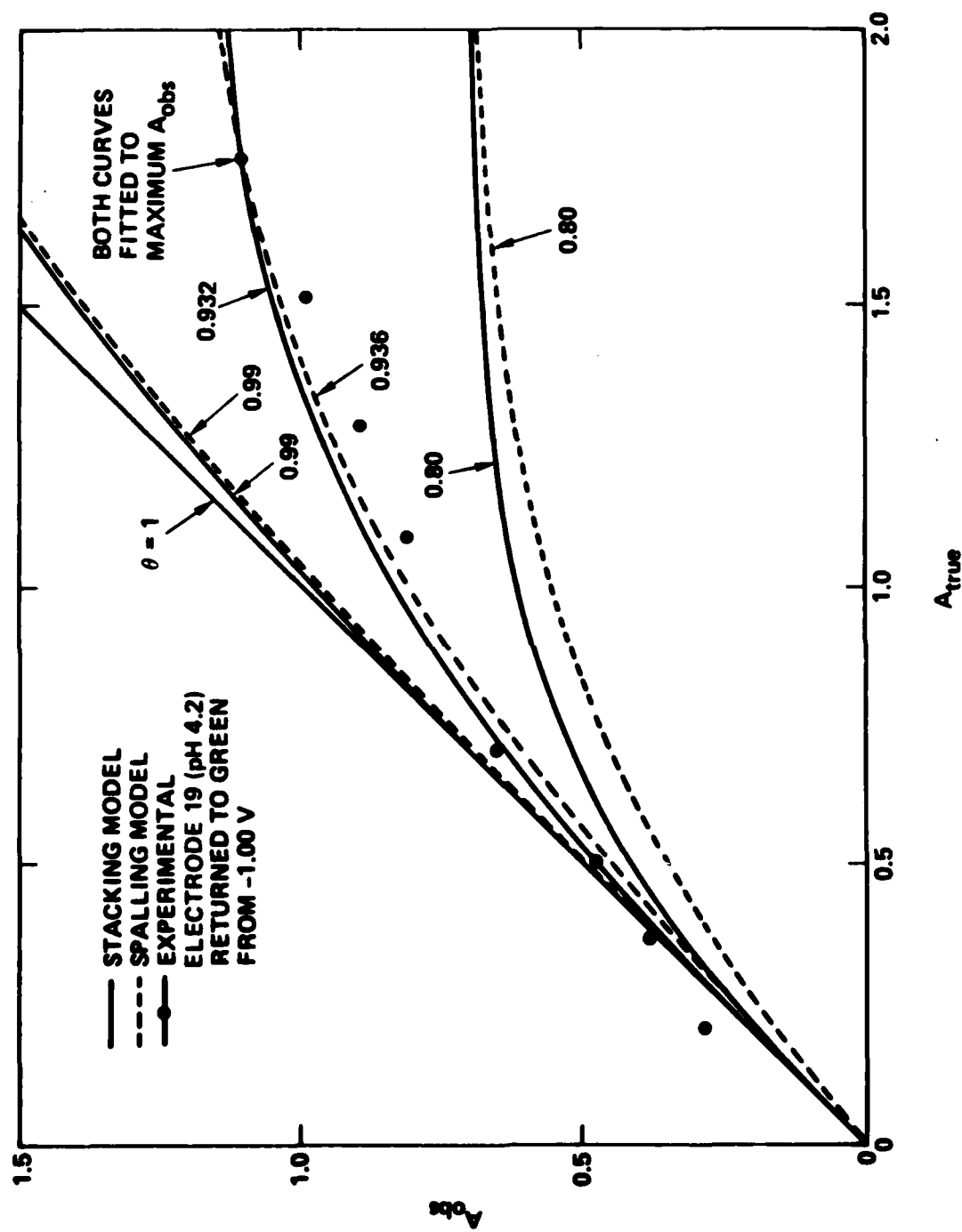


Figure 17. Relation of Observed Absorbance of Discontinuous Film to True Absorbance of Continuous Film

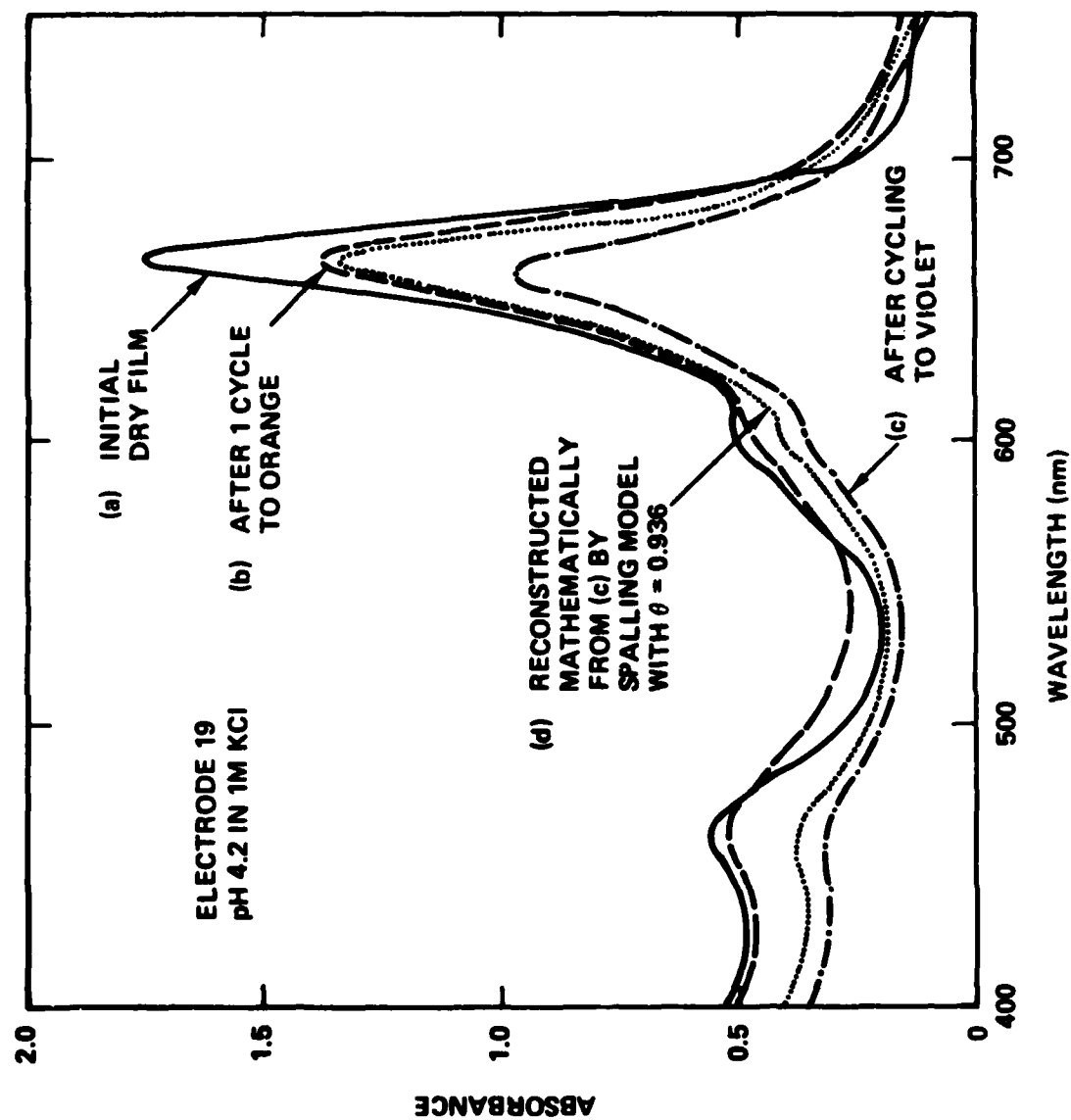


Figure 18. Spectra of Initial, Cycled, and Mathematically Reconstructed Green Film

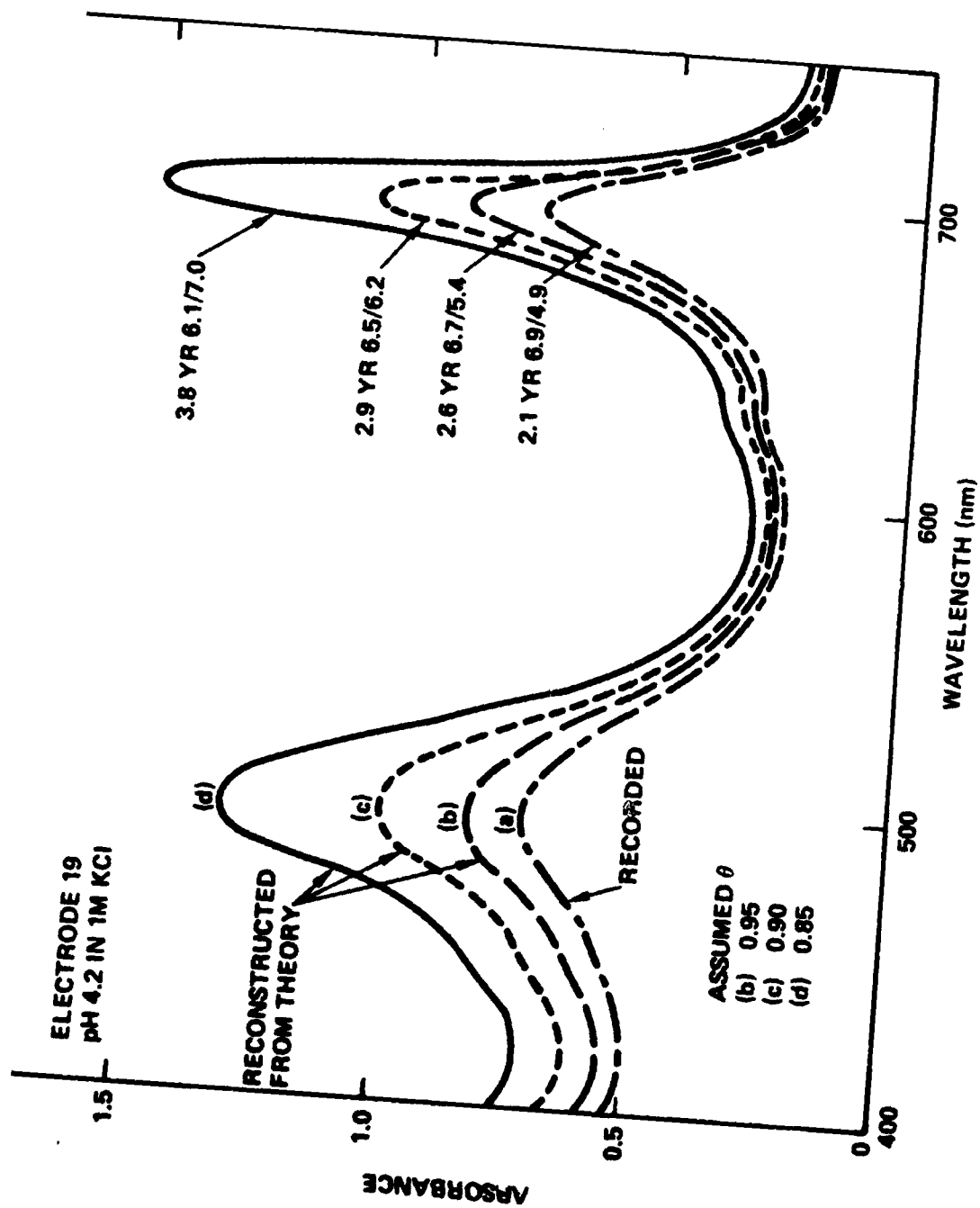


Figure 19. Recorded and Reconstructed Spectra of Cycled Orange Film

Other comments on the differences in orange and red states of the dye are given in Section III-C-2.

Explanation of Unusual Colors. Figure 20 illustrates a more dramatic effect of discontinuity on color. It was noted in Section III-A-3 that the violet at  $\text{pH} < 4$  differed from the violet at  $\text{pH} > 4$  and that the dark reduced film could be susceptible to hydrogen damage in the more acidic solutions. Curve (a) of Figure 20 is the experimental spectrum of a violet film at  $-0.55 \text{ V}$  in  $0.1 \text{ M HCl}$ . Curve (b) is a spectrum recorded at  $-1.00 \text{ V}$  for  $\text{pH} 1.3$  in  $1 \text{ M KCl}$ ; these conditions lie below the experimental hydrogen-evolution line in Figure 5. The color for (b) was almost neutral gray (10B 7/1). The broken line (c) was calculated from (a) for a 20% loss by spalling. The similarity of (b) and (c) is convincing evidence in support of the discontinuity model for a damaged film.

#### E. SUPPLEMENTARY ITEMS IN COLOR

Full-color charts constructed of standard matte-finish Munsell color materials corresponding to Figure 5 and other parts of the report are on file at the Office of Naval Research and at Rockwell International. A video tape was also made to show real-time color switching of an experimental cell used in this investigation.

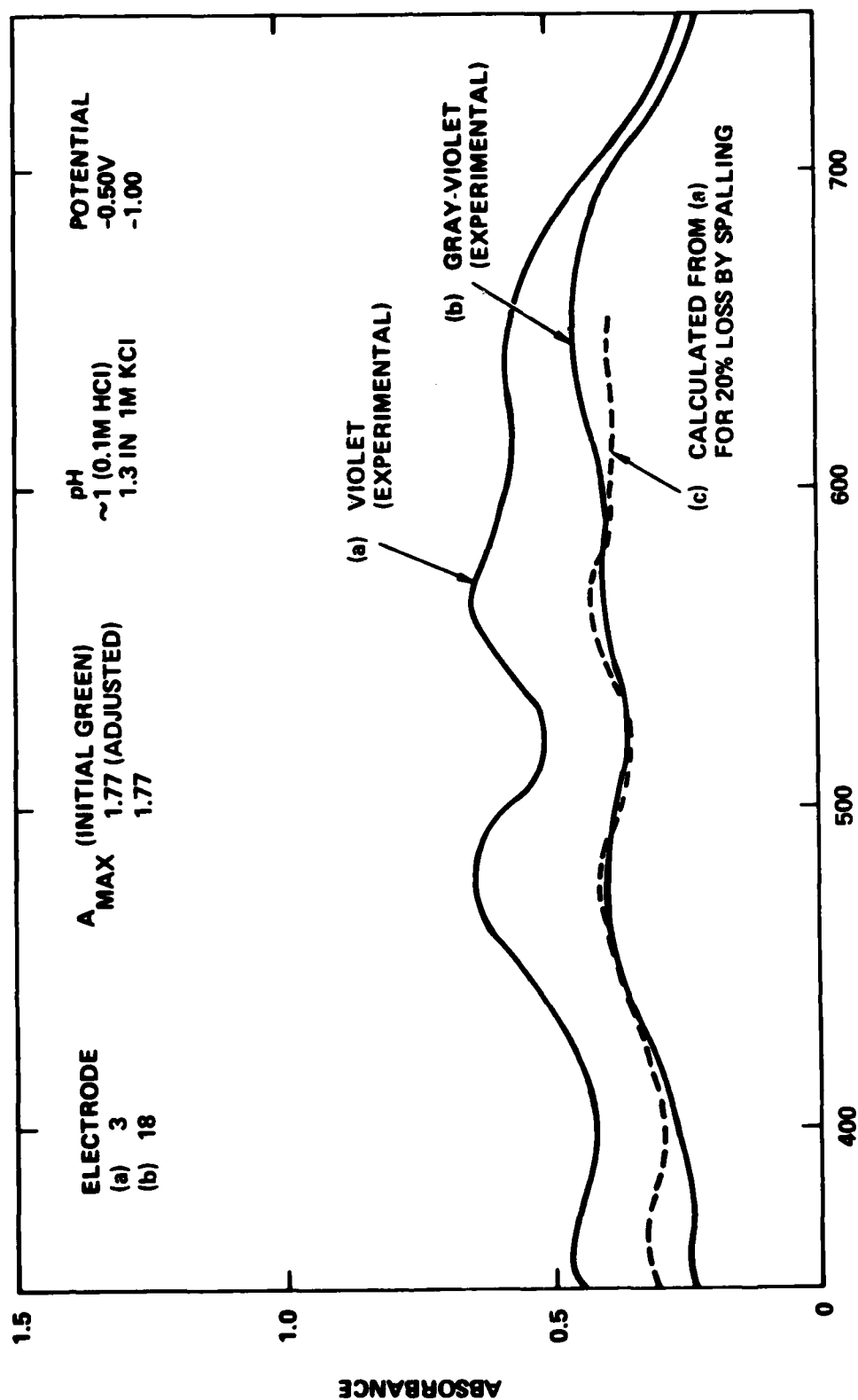


Figure 20. Observed and Mathematically Attenuated Spectra of Violet Films, Corresponding to Gray at 20 Percent Discontinuity

#### IV. CONCLUSIONS

The techniques and interpretive methods described here offer systematic approaches to further investigation of rare-earth diphthalocyanine electrochromic systems.

The pH is a primary variable affecting the colors, drive requirements, and cycle life of these display materials in aqueous media.

A pH-potential-color correlation chart developed from near-equilibrium measurements in chloride electrolytes defines the stability zones for the various color phases of lutetium diphthalocyanine and indicates where film damage due to side reactions could occur.

An electrochemical reaction scheme formulated from the slopes of lines on this chart and the charges measured for the corresponding color transitions is consistent in most details with reactions proposed in earlier studies by other methods. An unexpected result is the apparent formation of at least two acid adducts with reduction products of the dye. This indicates a broader dependence of the electrochromism on the electrolyte anion, which was only known previously to participate in the oxidation process.

Principal colors of the lutetium dye system in oxygen-free acidic chloride electrolytes are orange, green, light blue (two types), dark purple-blue (pH < 4), and violet. Yellows, blue-greens, and additional dark blues are results of blending the principal colors. This palette of the electrochromic display includes highly saturated colors and high-contrast color combinations.

Color modifications caused by discontinuities in the dye film are predicted by a simple mathematical model, which provides a method for assessment of film damage due to cracking and spalling. This model should be especially useful in further work to optimize the colors and extend the cycle life of diphthalocyanine electrochromic displays.

## V. ACKNOWLEDGMENTS

Acknowledgments are due to J. J. Duffy for assistance with the computer calculations and to T. J. Raab and Ronald Rushworth for analyses of the tin oxide films.

## VI. REFERENCES

1. M. M. Nicholson and R. V. Galiardi, "Investigation of Lutetium Diphthalocyanine as an Electrochromic Display Material," Final Report, Contract N62269-76-C-0574, C77-215/501, NADC-76283-30, May 1977, Rockwell International, Anaheim, California.
2. M. M. Nicholson and R. V. Galiardi, "A multicolor Electrochromic Display," SID International Symposium Digest, IX, 24 (1978).
3. G. A. Corker, B. Grant, and N. J. Clecak, "An Explanation of the Electrochromism of Lutetium Diphthalocyanine," J. Electrochem. Soc., 126, 1339 (1979).
4. M. M. Nicholson and F. A. Pizzarello, "Charge Transport in Oxidation Product of Lutetium Diphthalocyanine," J. Electrochem. Soc., 126, 1490 (1979).
5. M. Yamana, "Electrochromism of Er-Diphthalocyanine Complex," Ohyo Butsuri, 48, 441 (1979).
6. M. M. Nicholson and F. A. Pizzarello, "Galvanostatic Transients in Lutetium Diphthalocyanine Films," J. Electrochem. Soc., 127, 821 (1980).
7. F. A. Pizzarello and M. M. Nicholson, "Solid-State Anion Migration in the Anodic Oxidation of Lutetium Diphthalocyanine," J. Electron. Mater., 9, 231 (1980).
8. M. M. Nicholson and F. A. Pizzarello, "Effects of the Gaseous Environment on Propagation of Anodic Reaction Boundaries in Lutetium Diphthalocyanine Films," J. Electrochem. Soc., 127, 2617 (1980).
9. M. M. Nicholson, F. A. Pizzarello, and T. J. La Chapelle, "Multi-color Electrochromic Dot-Matrix Display Investigation," Final Report, Contract N00014-79-C-0434, ONR-CR339-005-1F, June 1980, Rockwell International, Anaheim, California.

10. F. A. Pizzarello and M. M. Nicholson, "Kinetics of Color Reversal in Lutetium Diphthalocyanine Oxidation Products Formed with Different Anions," J. Electrochem. Soc., 128, 1288 (1981).
11. M. M. Nicholson and F. A. Pizzarello, "Cathodic Electrochromism of Lutetium Diphthalocyanine," J. Electrochem. Soc., 128, 1740 (1981).
12. A. T. Chang and J.-C. Marchon, "Preparation and Characterization of Oxidized and Reduced Forms of Lutetium Diphthalocyanine," Inorg. Chim. Acta, 53, L241 (1981).
13. D. Walton, B. Ely, and G. Elliott, "Investigations into the Electrochromism of Lutetium and Ytterbium Diphthalocyanines," J. Electrochem. Soc., 128, 2479 (1981).
14. Y. Bessonat, G. Gerard, G. Leroy, and M. Le Contellec, "Improvement of Lutetium Diphthalocyanine Display Lifetime by Electrolyte Study," SID International Symposium Digest, XIII, 102 (1982).
15. M. M. Nicholson, "Lanthanide Diphthalocyanines. Electrochromism and Display Applications," Ind. Eng. Chem. Prod. R&D, 21, 261 (1982).
16. G. Wyszecki and W. Stiles, "Color Science: Concepts and Methods, Quantitative Data, and Formulas," Wiley, New York, 1967.
17. "Standard Method of Specifying Color by the Munsell System," ASTM Designation D 1535-68.
18. E. F. Trujillo, "Model DK-A Ratio Recording Spectrophotometers," Beckman Instruments, Fullerton, CA, 1963.
19. Munsell Book of Color, Neighboring Hues Edition, Matte Finish Collection, Macbeth Color and Photometry Division, Kollmorgen Corporation, New York, 1976.
20. M. Pourbaix et al., "Atlas d'Equilibres Electrochimiques," Gauthier-Villars, Paris, 1963.
21. R. N. Jones, "The Absorption of Radiation by Inhomogeneously Dispersed Systems," J. Am. Chem. Soc., 74, 2681 (1952).

## DISTRIBUTION

	<u>NUMBER OF COPIES</u>
Dr. Jerry J. Smith Office of Naval Research Code 472 800 North Quincy Arlington, VA 22217	2
Captain M. A. Howard Office of Naval Research Aviation and Aerospace Technology Code 210 800 North Quincy Arlington, VA 22217	1
Mr. Morris S. Solomon Contracting Officer Office of Naval Research 800 North Quincy Arlington, VA 22217	1
Director Naval Research Laboratory Code 2627 Washington, D.C. 20375	6
Defense Technical Information Center Building 5 Cameron Station Alexandria, VA 22314	12
Office of Naval Research Western Regional Office 1030 East Green Street Pasadena, CA 91106	1
Mr. W. G. Mulley Naval Air Development Center Code 54P3 Warminster, PA 18974	1

	<u>NUMBER OF COPIES</u>
Mr. George Tsaparas Naval Air Systems Command Code AIR-340D Washington, D.C. 20361	1
Mr. Phillip J. Andrews Naval Sea Systems Command Code NAVSEA 61R2 Washington, D.C. 20362	1
Mr. Joseph Terek Washington, D.C. 20505	1
Dr. A. J. Matuszko Directorate of Chemical and Atmospheric Sciences Air Force Office of Scientific Research (AFSC) Bolling Air Force Base, D.C. 20332	1
Mr. Joseph Nesci Rome Air Development Center Command and Control Division, COTA Griffiss Air Force Base, N.Y. 13441	1
Mr. John F. Dove Rome Air Development Center Command and Control Division, COTA Griffiss Air Force Base, N.Y. 13441	1
Lt. Gregory Swietek Rome Air Development Center Surveillance Division, OCDS Griffiss Air Force Base, N.Y. 13441	1
Mr. John O. Mysing Air Force Avionics Laboratory AFWAL/AAT-1 Wright-Patterson Air Force Base, OH 45433	1

NUMBER OF COPIES

Dr. Keith T. Burnette 1  
Bunker Ramo Corporation  
AFWAL/FIGR  
Wright-Patterson Air Force Base, OH 45433

Mr. Walter Melnick 1  
Air Force Flight Dynamics Laboratory  
AFWAL/FIGR  
Wright-Patterson Air Force Base, OH 45433

Dr. Issai Lefkowitz 1  
U.S. Army Research Office  
P. O. Box 12211  
Research Triangle Park, NC 27709

Dr. Bernard F. Spielvogel 1  
U.S. Army Research Office  
P. O. Box 12211  
Research Triangle Park, NC 27709

Dr. Elliott Schlam 1  
U.S. Army Electronics Research and Development Command  
Electronics Technology and Devices Laboratory  
Ft. Monmouth, NJ 07703

Mr. Charles Askew 1  
U.S. Army Communicative Technology Office  
P. O. Box 4337  
Ft. Eustis, VA 23604

Mr. Jack J. Hatfield 1  
Cockpit Systems Branch  
Flight Control Systems Division  
NASA Langley Research Center  
Hampton, VA 23665

**END**

**FILMED**